Available online at www.sciencedirect.com
ScienceDirect
Marine Chemistry 105 (2007) 30–51
MARINE CHEMISTRY
www.elsevier.com/locate/marchem

The effect of biogeochemical processes on pH

Karline Soetaert [a,*], Andreas F. Hofmann [a], Jack J. Middelburg [a], Filip J.R. Meysman [a], Jim Greenwood [a,b]

[a] *Netherlands Institute of Ecology (NIOO-KNAW), Centre for Estuarine and Marine Ecology, POB 140, 4400 NT Yerseke, The Netherlands*
[b] *CSIRO Marine and Atmospheric Research, Underwood Ave., Floreat 6014, Western Australia*

Received 29 September 2005; received in revised form 31 October 2006; accepted 12 December 2006
Available online 20 December 2006

Abstract

The impact of biogeochemical and physical processes on aquatic chemistry is usually expressed in terms of alkalinity. Here we show how to directly calculate the effect of single processes on pH. Under the assumptions of equilibrium and electroneutrality, the rate of change of pH can be calculated as the product of (1) the net charge exchanged during the process and (2) the consequent buffering of pH variations. As both the chemical buffering and the charge of reactive species changes with pH, so does the effect of biogeochemical processes depend on pH.

We calculate the effect on pH for a variety of biogeochemical processes, typical for both the water column and sediments, and for a pH range of 2–12. Four different response patterns emerge. (1) Some processes, e.g. nitrate assimilation, iron and manganese reduction, and calcite dissolution monotonically tend towards higher pH. (2) Other processes, e.g. calcification and most oxidation reactions monotonically lower the pH. (3) Most respiration reactions and the anaerobic oxidation of methane (AOM) converge to a pH between 5.2 (aerobic respiration) and 7.9 (AOM). (4) Ammonium assimilation and the anaerobic ammonium oxidation (ANAMMOX) either tend to very low or very high pH, depending on initial conditions, i.e. pH diverges away from an unstable neutral point, at pH 5.2 and 7.1 respectively. Similar response patterns are observed when the effects of combinations of processes are considered.

We discuss two general applications of our approach. (1) Biogenic calcification (C) coupled to photosynthetic production (P) is a type 4 process, with pH diverging from an unstable neutral point. (2) On the long-term, the AOM converges pH to values that are high enough to enable calcification. This contrasts to sulphate reduction, where the equilibrium pH is too low for calcification. This explains the strong linkage between AOM and carbonate formation, whilst sulphate reduction, unless it is followed by sulphide precipitation does generally not lead to calcification.

The method is not intended to replace complex transport-reaction modelling where accurate prediction of the pH is desired.

Keywords: pH; Buffer intensity; Biochemistry; Water column; Sediment; Calcification

1. Introduction

Protons in solution are affected both through biogeochemical and physical processes that directly consume or release protons and through reactions that buffer their variations. Under natural conditions, seawater has a large capacity to neutralize protons and therefore to buffer pH variations (Stumm and Morgan, 1981). This buffering capacity is mainly attributable to weak bases such as HCO_3^-, CO_3^{2-}, borates, and to a lesser extent to OH^-, as well as to species often present

* Corresponding author.
E-mail address: k.soetaert@nioo.knaw.nl (K. Soetaert).

0304-4203/$ - see front matter © 2007 Elsevier B.V. All rights reserved.
doi:10.1016/j.marchem.2006.12.012

in small concentrations such as phosphates, ammonia, silicates (Broecker and Peng, 1982), or organic bases (Cai et al., 1998). Most of these species are also actively produced and/or consumed during biogeochemical processes. The complex interactions between the biogeochemical and physical processes that produce acids (including protons) or bases, with chemical equilibria that buffer pH, obscure the biogeochemical interpretation of pH variations.

It is partly due to this complexity that the impact of biogeochemical processes on the chemical environment is usually expressed in terms of alkalinity. Dickson (1981) defines alkalinity as the number of moles of hydrogen ion equivalent to the excess of proton acceptors (bases formed from weak acids with a dissociation constant $K \leq 10^{-4.5}$ at 25 °C and zero ionic strength) over proton donors (acids with $K > 10^{-4.5}$) in one kg of sample. As the quantity is not affected by the chemical equilibrium reactions (Zeebe and Wolf-Gladrow, 2001), alkalinity changes are easily interpreted as resulting from consumption, production, or transport. Moreover, as alkalinity records different processes than for instance dissolved inorganic carbon (DIC), it can be used as an indicator of specific biogeochemical processes. For instance, it is only marginally affected by aerobic, but strongly affected by anaerobic respiration. Therefore, in sediment systems, alkalinity can be used as an integrated measure of anaerobic processes (Cai and Wang, 1998). Calcification decreases alkalinity twice as much as it affects DIC, such that in the water column, concurrent changes in alkalinity and DIC are used as indicators of calcite production or dissolution and of community respiration (Smith and Key, 1975; Gattuso et al., 1999).

Once alkalinity is known, it is relatively straightforward to calculate pH, given that either total dissolved inorganic carbon concentration or carbon dioxide fugacity ($\sim CO_2$ partial pressure) is known together with the relevant acid dissociation constants (Park, 1969), and the total concentrations of acid/base components other than carbonates. It is also relatively straightforward to estimate the effect of processes on alkalinity: it can be inferred from reaction stoichiometry. However, it is less straightforward to calculate effects of biogeochemical processes on pH or on single acids or bases via their impact on alkalinity. This is because, although pH and alkalinity are related, they can change independently from one another. For instance, air–sea exchange of carbon dioxide does not affect alkalinity, but has an effect on pH. Nitrification and calcification have similar effect on alkalinity, but dissimilar effects on pH.

Moreover, the effect of biogeochemical processes on pH or on single acids and bases depends on pH itself. This complicates our writing of chemical reactions, which are consistent for alkalinity, but only approximately true for single acid and base species. Consider for instance two ways to write the calcification reaction:

$$Ca^{2+} + 2HCO_3^- \rightarrow CaCO_3 + CO_2 + H_2O$$

$$Ca^{2+} + CO_3^{2-} \rightarrow CaCO_3$$

Both equations are consistent with respect to their effects on inorganic carbon (1 mole consumed) and alkalinity (2 moles consumed). However, the former reaction also suggests that one mole of CO_2 is formed, whilst the second reaction does not. As shown experimentally (Wollast et al., 1980), and by numerical (Ware et al., 1991) and analytical calculations (Frankignoulle et al., 1994), none of these equations is universally correct, as neither takes into account chemical re-equilibration (Copin Montégut and Copin Montégut, 1999). Indeed, under typical oceanic conditions, CO_2 will be exchanged with the atmosphere in a ratio of about 0.6 moles of CO_2 per mole of $CaCO_3$ deposited and this ratio changes with pH, pCO_2, and temperature and salinity of the water (Frankignoulle et al., 1994). Thus, to estimate the true molar ratio of CO_2 produced per carbonate formed, a complex formula needs to be applied, that takes into account the pH, temperature and salinity at which the reaction occurs (Frankignoulle, 1994; Frankignoulle et al., 1994).

Inspired by Frankignoulle's 1994 papers, we present a general approach to quantify the impact of single and ensemble biogeochemical processes on pH. We first discuss the various acid–base reactions that are important in the marine environment and that are considered to operate at equilibrium. We then deal with a large number of biogeochemical (e.g. primary production, mineralization) and physical (e.g. air–sea exchange) processes that occur at much lower rates. We quantify the impacts of these single processes on pH and for a wide pH range between 2 and 12. Although under most conditions, pH is kept into a typical range of ($\sim$7–8.3), much more extreme pH values have been found in various environments including animal guts and eutrophic freshwater bodies (pH > 10; Jeppesen et al., 1998) and in groundwater and lakes receiving drainage water from mines (pH < 4; Ferris et al., 2004). Moreover, pH gradients between pH 5 and 9 have been measured in brine channels in sea ice (Bronshteyn and Chernov, 1991; Gleitz et al., 1995). As we also consider anaerobic processes, our approach is relevant for sediments, as

Table 1
Concentrations of the acid–base components as used in the model runs, and their mean charge ($\bar{X}$*) at pH 8.2 (on free scale), temperature 25 °C, salinity 35 and 1 atm pressure

Species lump sum $\sum X$	Concentration [10^{-6} mol kg^{-1}]	$\bar{X}$*
$\Sigma B(OH)_4$	416	−0.24
ΣF	68	−1.0
ΣSO_4	28235	−2.0
ΣCO_2 [a]	2100	−1.12
ΣPO_4	2	−2.16
ΣNO_3	31	−1.0
ΣNO_2	0.1	−1.0
ΣNH_3	1.0	+0.94
ΣSiO_4	4.0	−0.05
ΣS	0.1	−0.97
$\Sigma[-]$	59039	
Talk	2466	
Density (kg m^{-3})	1023.3	

[a] Total inorganic carbon was estimated such that at pH 8.2, temperature 25 °C, salinity 35 and 1 atm pressure, the pCO_2 was 364 μatm.

well as for water-column processes, including those in anoxic basins such as the Black-Sea, Namibia shelf etc. However, we do not exhaustively deal with solid–liquid interactions, e.g. sediment buffering via Fe-oxides. Note that, as the method considers the effect of single processes, it is not intended to replace complex transport-reaction modelling where accurate prediction of the pH is desired. It is also inaccurate when there are effects of differential transport rates between protolytic species, such as in sediments.

2. Material and methods

Calculations were performed in the simulation environment Femme (Soetaert et al., 2002). The model will be made downloadable from the femme webpage (http://www.nioo.knaw.nl/ceme/femme). All analytical solutions were checked against their numerical counterparts, i.e. by differencing perturbed and reference solutions.

The stoichiometric equilibrium constants were calculated as a function of temperature, salinity, and pressure as in Millero (1995) with typographical correction from CO2SYS (Lewis and Wallace, 1998); they are expressed on the free pH scale. The constant for the dissociation of HS^- was taken as 10^{-18} mol kg^{-1} solution (Schoonen and Barnes, 1988), which effectively annihilates S^{2-} production. It was also assumed that $[H_2SO_4]=0$ (pK much below 2). The dissociation constant for nitrate was set to 23.44 mol kg^{-1} solution (Boudreau, 1996), which also implies that $[HNO_3]=0$ for the pH range considered. For nitrite, a dissociation constant of 4.5 10^{-4} mol kg^{-1} for freshwater and 25 °C was used; to convert to prevailing environmental conditions, we used the same salinity and temperature dependence factors as for fluoride. The dissociation of water is expressed in terms of the 'ion product of water, K_W', which equals the equilibrium constant times the (constant) concentration of water.

Where required, conversion from volumetric to weight-specific concentrations was performed using the density of seawater, calculated as a function of salinity and temperature. All calculations were

Notes to Table 2:
Species in brackets represent total concentrations, per kg solution; proton concentration is expressed in the same units as the dissociation constants (mol kg^{-1} solution), except for K_W (mol^2 kg^{-2}). Values of the equilibrium constants are on the free pH scale and defined at 25 °C, salinity 35, and pressure of 1 atm. They are based on Millero (1995) with corrections by Lewis and Wallace (1998).
Where:

$$\Sigma CO_2 = [CO_2] + [HCO_3^-] + [CO_3^{2-}]$$

$$\Sigma B(OH)_4 = [B(OH)_3] + [B(OH)_4^-]$$

$$\Sigma PO_4 = [H_3PO_4] + [H_2PO_4^-] + [HPO_4^{2-}] + [PO_4^{3-}]$$

$$\Sigma SiO_4 = [H_4SiO_4] + [H_3SiO_4^-] + [H_2SiO_4^{2-}]$$

$$\Sigma NH_3 = [NH_4^+] + [NH_3]$$

$$\Sigma NO_3 = [HNO_3] + [NO_3^-] = [NO_3^-]$$

$$\Sigma NO_2 = [HNO_2] + [NO_2^-]$$

$$\Sigma SO_4 = [H_2SO_4] + [HSO_4^-] + [SO_4^{2-}] = [HSO_4^-] + [SO_4^{2-}]$$

$$\Sigma F = [HF] + [F^-]$$

$$\Sigma S = [H_2S] + [HS^-] + [S^{2-}] = [H_2S] + [HS^-]$$

Table 2
Main chemical reactions that affect pH, the thermodynamic constants and the equilibrium concentrations

	Reaction	ct	Equilibrium concentration
1a	$CO_2 + H_2O \Leftrightarrow H^+ + HCO_3^-$	$K_{C1}\ 0.11\times10^{-5}$	$[HCO_3^-] = \frac{K_{C1}\cdot[H^+]}{[H^+]\cdot[H^+] + K_{C1}\cdot[H^+] + K_{C1}\cdot K_{C2}}\cdot\Sigma CO_2$
1b	$HCO_3^- \Leftrightarrow H^+ + CO_3^-$	$K_{C2}\ 0.93\times10^{-9}$	$[CO_3] = \frac{K_{C1}\cdot K_{C2}}{[H^+]\cdot[H^+] + K_{C1}\cdot[H^+] + K_{C1}\cdot K_{C2}}\cdot\Sigma CO_2$
2	$H_2O \Leftrightarrow H^+ + OH^-$	$K_W\ 0.46\times10^{-13}$	$[OH^-] = \frac{K_W}{[H^+]}$
3	$B(OH)_3 + H_2O \Leftrightarrow H^+ + B(OH)_4^-$	$K_B\ 0.20\times10^{-8}$	$[B(OH)_4^-] = \frac{K_B}{H^+ + K_B}\cdot\sum B(OH)_4$
4a	$H_3PO_4 \Leftrightarrow H^+ + H_2PO_4^-$	$K_{P1}\ 0.19\times10^{-1}$	$[H_2PO_4^-] = \frac{K_{P1}\cdot[H^+]^2}{[H^+]^3 + [H^+]^2K_{P1} + [H^+]\cdot K_{P1}\cdot K_{P2} + K_{P1}\cdot K_{P2}\cdot K_{P3}}\cdot\sum PO_4$
4b	$H_2PO_4^- \Leftrightarrow H^+ + HPO_4^{2-}$	$K_{P2}\ 0.85\times10^{-6}$	$[HPO_4^{2-}] = \frac{K_{P1}\cdot K_{P2}\cdot[H^+]}{[H^+]^3 + [H^+]^2K_{P1} + [H^+]K_{P1}K_{P2} + K_{P1}K_{P2}K_{P3}}\cdot\sum PO_4$
4c	$HPO_4^{--} \Leftrightarrow H^+ + PO_4^{3-}$	$K_{P3}\ 0.13\times10^{-8}$	$[PO_4^{3-}] = \frac{K_{P1}\cdot K_{P2}\cdot K_{P3}}{[H^+]^3 + [H^+]^2K_{P1} + [H^+]\cdot K_{P1}\cdot K_{P2} + K_{P1}\cdot K_{P2}\cdot K_{P3}}\cdot\sum PO_4$
5a	$H_4SiO_4 \Leftrightarrow H^+ + H_3SiO_4^-$	$K_{Si1}\ 0.31\times10^{-9}$	$[H_3SiO_4^-] = \frac{K_{Si1}\cdot[H^+]}{[H^+]\cdot[H^+] + [H^+]\cdot K_{Si1} + K_{Si1}\cdot K_{Si2}}\cdot\sum SiO_4$
5b	$H_3SiO_4^- \Leftrightarrow H^+ + H_2SiO_4^{2-}$	$K_{Si2}\ 0.12\times10^{-12}$	$[H_2SiO_4^{2-}] = \frac{K_{Si1}\cdot K_{Si2}}{[H^+]\cdot[H^+] + [H^+]\cdot K_{Si1} + K_{Si1}\cdot K_{Si2}}\cdot\sum SiO_4$
6	$NH_4^+ \Leftrightarrow H^+ + NH_3$	$K_N\ 0.42\times10^{-9}$	$[NH_3] = \frac{K_N}{[H^+] + K_N}\cdot\sum NH_x$
7	$HNO_3 \Rightarrow H^+ + NO_3^-$	$K_{NO_3}\ 0.23\times10^{2}$	$[HNO_3] = 0$
8a	$H_2SO_4 \Rightarrow H^+ + HSO_4^-$	$K_{H_2SO_4}\ \infty$	$[H_2SO_4] = 0$
8b	$HSO_4^- \Leftrightarrow H^+ + SO_4^{2-}$	$K_{So}\ 0.10$	$[SO_4^{2-}] = \frac{K_{So}}{[H^+] + K_{So}}\cdot\sum SO_4$
9	$HF \Leftrightarrow H^+ + F^-$	$K_F\ 0.24\times10^{-2}$	$[F^-] = \frac{K_F}{[H^+] + K_F}\cdot\sum F$
10a	$H_2S \Leftrightarrow H^+ + HS^-$	$K_{S1}\ 0.24\times10^{-6}$	$[HS^-] = \frac{K_{S1}\cdot[H^+]}{[H^+]\cdot[H^+] + K_{S1}\cdot[H^+] + K_{S1}\cdot K_{S2}}\cdot\sum S$
10b	$HS^- \Leftarrow H^+ + S^{2-}$	$K_{S2}\ 1.0\times10^{-18}$	$[S^{2-}] = 0$
11	$HNO_2 \Leftrightarrow H^+ + NO_2^-$	$KNO_2\ 0.12\times10^{-4}$	$[NO_2^-] = \frac{K_{No2}}{[H^+] + K_{No2}}\cdot\sum NO_2$

performed at 25 °C, salinity 35, 1 atm pressure, either for a pH range of [2–12] or for a pH of 8.2 (on the free scale). The DIC concentration was tuned such that the pCO_2 was about 360 μatm. The borate, fluoride and sulphate concentrations were calculated as a function of salinity as described in Millero (1995), Riley (1965) and Morris and Riley (1966) respectively. For the concentrations of the lesser species we chose values typical for the Atlantic Ocean. The environmental concentrations used in the calculations are in Table 1.

3. Acid–base reactions

Acid–base reactions are reversible chemical reactions that involve the uptake or release of a proton. They can be formalised by the following:

$$H_iX^{i-a} \leftrightarrow H_{i-l}X^{i-a-1} + H^+ \quad i = 1, \ldots a$$

where i is the number of protons, a is the maximal charge, H_iX^{i-a} is an acid, and $H_{i-1}X^{i-a-1}$ is its conjugated base. The acid–base reactions that can affect the pH in a range of [2–12], and which are important in seawater are given in Table 2. They are the dissociation and protonation of carbonates (Eq. (1a) (1b)), water (Eq. (2)), borate (Eq. (3)), phosphates (Eqs. (4a) (4b) (4c)), silicates (Eqs. (5a) and (5b)), ammonium (Eq. (6)), nitrate (Eq. (7)), sulphate (Eqs. (8a) and (8b)), fluoride (Eq. (9)), sulphide (Eq. (10a) (10b)), and nitrite (Eq. (11)). Sulphide was included as it can reach high concentrations in anoxic water basins (de Lange et al., 1990), in certain sediments (Ben-Yaakov, 1973) and in groundwater (Hunter et al., 1998). Nitrite was added because of its role in the ANAMMOX reaction.

3.1. Equilibrium assumption

The acid–base reactions generally occur at rates which, compared to the slow biogeochemical reactions that consume or produce protons, are sufficiently fast, such that they can be considered to operate at equilibrium (e.g. Wolf-Gladrow and Riebesell, 1997). At equilibrium, the speciation of acids and bases can be written as (Zeebe and Wolf-Gladrow, 2001):

$$[H_{i-1}X^{i-a-1}] = K_{H_{i-1}X^{i-a-1}} \cdot \frac{[H_iX^{i-a}]}{[H^+]},$$

where $K_{H_{i-1}X^{i-a-1}}$ is the 'stoichiometric equilibrium constant', expressed in mol (kg solution)$^{-1}$.

It is common practice to express the stoichiometric equilibrium speciation in terms of the total concentrations of species ($\Sigma X = \sum_i [H_iX^{i-a}]$), rather than considering the single species. These lump sums of concentrations (ΣX) are measured with most analytical techniques and are generally used in biogeochemical models. The lump sum concentrations are *not* affected by the chemical equilibrium reactions from Table 2.

The equilibrium concentrations of the acid–base species and the values for the stoichiometric equilibrium constants (25 °C, salinity 35, pressure 1 atm) are in Table 2. In all calculations the temperature, salinity and pressure are kept constant.

3.2. Solving for the equilibrium pH

To solve for the pH at equilibrium, the concentrations of all the ions ($[HCO_3^-]$, $[CO_3^{2-}]$, …) and the proton concentration $[H^+]$ have to be calculated simultaneously, based on the formulations for the equilibrium concentration of all the acid–base species, the lump sums of concentrations and the values of the equilibrium constants (Table 2). As there are 17 unknowns, one more than the number of equations, an extra equation is required to find a unique solution. The equations are therefore completed by describing some form of charge or proton balance. This balance must be independent from the other equations and should not be affected by any of the acid–base reactions in Table 2. There exist many different ways in which to compile such a quantity.

One straightforward measure consists of the total acid–base reactivity of the solution, hereafter referred to as 'excess negative charge' and denoted by $\Sigma[-]$. This quantity expresses the moles of negative charges over positive charges of the acid–base system given in Table 2. Thus, from Table 2, all the concentrations of negative ions minus the positive ones and multiplied by their charge are listed:

$$\begin{aligned}\Sigma[-] = {} & [HCO_3^-] + 2[CO_3^{2-}] + [OH^-] + [B(OH)_4^-] \\ & + [H_2PO_4^-] + 2[HPO_4^{2-}] + 3[PO_4^{3-}] + [H_3SiO_4^-] \\ & + 2[H_2SiO_4^{2-}] + [NO_3^-] + [NO_2^-] + [F^-] \\ & + [HS^-] + 2[S^{2-}] + [HSO_4^-] \\ & + 2[SO_4^{2-}] - [NH_4^+] - [H^+].\end{aligned}$$

The most commonly used measure of proton balance is total alkalinity (TA). According to the definition of Dickson (1981), TA is the number of moles of hydrogen ion equivalent to the excess of proton acceptors (bases formed from weak acids with a dissociation constant $K \leq 10^{-4.5}$ at 25 °C and zero ionic strength) over proton

donors (acids with $K > 10^{-4.5}$) in 1 kg of sample. Based on the chemical reactions and dissociation constants from Table 2 we obtain:

$$\begin{aligned} TA = {} & [HCO_3^-] + 2[CO_3^{2-}] + [OH^-] + [B(OH)_4^-] \\ & + [HPO_4^{2-}] + 2[PO_4^{3-}] + [H_3SiO_4^-] + 2[H_2SiO_4^{2-}] \\ & + [NH_3] + [HS^-] + 2[S^{2-}] - [H^+] - [H_3PO_4] \\ & - [HSO_4^-] - [HF] - [HNO_3] - [HNO_2] - 2[H_2SO_4] \end{aligned}$$

and where $[HNO_3]$ and $[H_2SO_4]$ are 0 for the pH range considered.

This quantity (or part of it), is most often used in marine biogeochemical models, both in the pelagic (e.g. Taylor et al., 1992; Follows et al., 1996) or in the sediment (e.g. Boudreau and Canfield, 1993, Van Cappellen and Wang, 1996; Meysman et al., 2003).

We use excess negative charge rather than the total alkalinity concept for a number of reasons. First of all, if we assume that uptake of ions is compensated by uptake or release of protons (electroneutrality, see below), then $\Sigma[-]$ is not impacted by changes in the concentrations of nitrate, nitrite, phosphate, ammonia/ammonium, sulphate nor fluoride. In contrast, total alkalinity is increased by production of ammonium, decreased by the production of nitrate, nitrite, phosphate and fluoride. Moreover, it is affected doubly by sulphate. Finally, it is straightforward to convert the excess negative charge to total alkalinity:

$$\begin{aligned} TA = {} & \Sigma[-] + \Sigma NH_3 - \Sigma NO_3 - \Sigma NO_2 \\ & - \Sigma PO_4 - 2\Sigma SO_4 - \Sigma F \end{aligned}$$

The complete system of equations can be solved using a non-linear root-finding procedure, such as the Newton–Raphson technique or Brent's method (Press et al., 1997) for the concentration of H^+ and pH.

3.3. The mean and total charge of acid–base species

The total (X^*) and mean negative charge ($\bar{X}^*$) of a species ($\Sigma X = \sum_i [H_i X^{i-a}]$) is the sum, respectively average, of the concentration of the different ions, weighted for their charge (Ben-Yaakov, 1973):

$$X^* = \sum_i (i-a) H_i X^{i-a}$$

$$\bar{X}^* = \frac{\sum_i (i-a) H_i X^{i-a}}{\sum_i H_i X^{i-a}}$$

For instance, using the equations from Table 2, the mean charge of dissolved inorganic carbon (ΣCO_2) is given by:

$$\begin{aligned} \overline{CO_2}^* &= \frac{-[HCO_3^-] - 2[CO_3^{2-}]}{\sum CO_2} \\ &= \frac{-K_{C1} \cdot [H^+] - 2 \cdot K_{C1} \cdot K_{C2}}{[H^+] \cdot [H^+] + K_{C1} \cdot [H^+] + K_{C1} \cdot K_{C2}} \end{aligned}$$

The excess negative charge ($\Sigma[-]$) can now be written as the negative of the sum of the total charge of all the acid–base species:

$$\Sigma[-] = -\sum_x X^*$$

As is clear from the equilibrium concentrations (Table 2), the speciation of the acid–base components changes as a function of the proton concentration. Assuming a constant temperature, salinity and pressure, the mean charge ($\bar{X}^*$) thus only depends on pH. Fig. 1A depicts the speciation and mean charge of dissolved inorganic carbon, as a function of pH, and estimated at the reference environmental conditions. When all DIC is in the form of carbon dioxide (CO_2), its mean charge is 0; when all is carbonate (CO_3^{2-}), its mean charge is −2. At increasing pH (decreasing H^+ concentration), the equilibrium shifts towards more negatively charged ions. At pH ~ 7.5, DIC has mean charge = −1; above that pH it is more negatively charged (Fig. 1A).

In Fig. 1B the mean charges of *all* acid–base components from Table 2, are plotted as a function of pH. Above pH ~ 7, phosphates have highest negative charge; below that pH, sulphates are more dissociated. Nitrates, sulphates and fluorides are for more than 99% dissociated above pH 0.7, 2.7 and 4.6 respectively. Borate, ammonium and silicates dissociate (>1%) above pH 6.7, 7.4, and 7.8 respectively. Nitrite is for 1% and 99% charged at a pH of 2.9 and 6.9 respectively. DIC and sulphides become charged (>1%) above pH 4.3 and 4.6 respectively.

3.4. The buffering capacity of the solution

In order to significantly buffer pH variations, species must have both high concentrations and the capacity to accept or release protons at the current pH.

The buffering capacity of an acid–base component ($\sum X$) can be estimated as the change of its total charge (X^*) induced by proton removal (Stumm and Morgan,

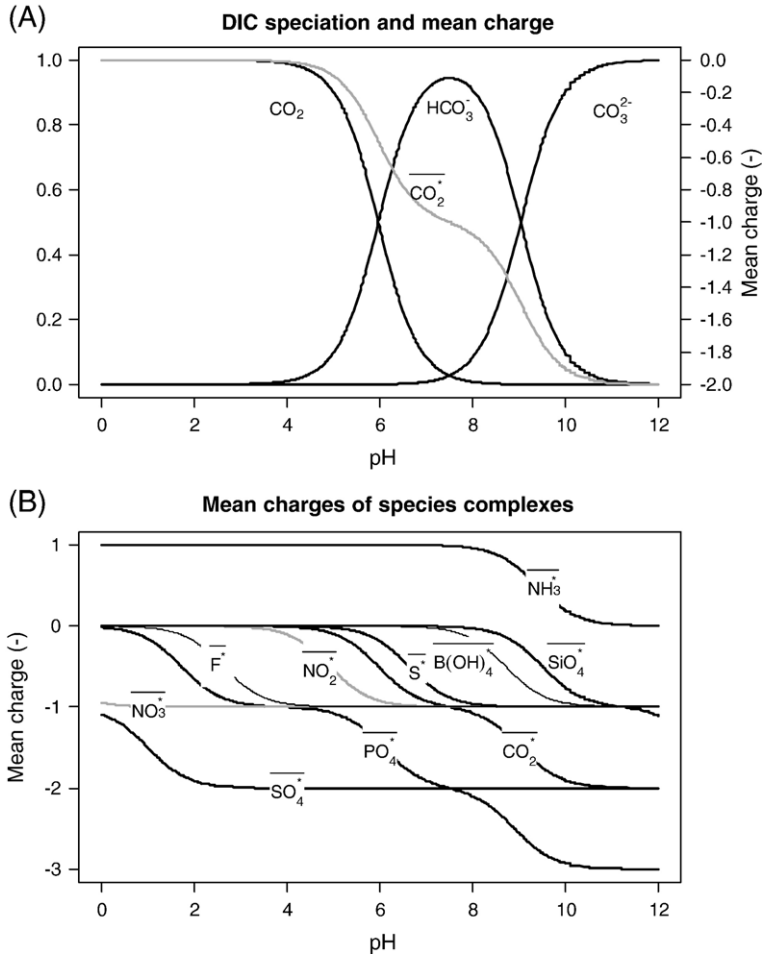

Fig. 1. A. Relative contribution of the acid–base components of dissolved inorganic carbon (ΣCO_2), and the mean charge ($\overline{CO_2^*}$) as a function of pH and at 25 °C, salinity 35 and pressure 1 atm. B. Mean charges of all species (see text for its calculation).

1981), i.e. by $\left(-\frac{\partial X^*}{\partial [H^+]}|_{\sum X=\mathrm{ct}}\right)$. The capacity for DIC to buffer H^+ and pH variations is thus estimated as:

$$-\left.\frac{\partial CO_2^*}{\partial [H^+]}\right|_{\sum CO_2=\mathrm{ct}} = \left.\frac{\partial([HCO_3^-]+2[CO_3^{2-}])}{\partial [H^+]}\right|_{\sum CO_2=\mathrm{ct}}$$

and

$$\left.\frac{\partial CO_2^*}{\partial \mathrm{pH}}\right|_{\sum CO_2=\mathrm{ct}} = -\frac{[H^+]}{\log_{10}(e)} \cdot \left.\frac{\partial CO_2^*}{\partial [H^+]}\right|_{\sum CO_2=\mathrm{ct}}.$$

These quantities can be calculated by substituting the bicarbonate and carbonate concentration by the formulae from Table 2. The derivatives with respect to $[H^+]$ are in the Appendix.

The buffering capacity of the solution is the sum of the buffering capacity of all acid–base components:

$$\left.\frac{\partial \sum[-]}{\partial [H^+]}\right|_{\sum X=\mathrm{ct}} = -\sum_x \frac{\partial X^*}{\partial [H^+]}$$

$$\left.\frac{\partial \sum[-]}{\partial \mathrm{pH}}\right|_{\sum X=\mathrm{ct}} = \frac{[H^+]}{\log_{10}(e)} \cdot \sum_x \frac{\partial X^*}{\partial [H^+]}.$$

And where ΣX=ct denotes that all lump-summed concentrations are assumed constant. These quantities estimate the effect on the total buffer concentration induced by a certain pH change. They can easily be derived analytically (Appendix).

The total buffering capacity, obtained by summing over the various acid–base species, and under the

reference conditions (as in Table 1), amounts to 760 μmol kg^{-1} [pH unit]$^{-1}$.

3.5. The chemical buffer factors

The inverse of the buffering capacity is often called the chemical buffer factor. It quantifies the effect of adding negative charge (e.g. via a strong base) on protons or pH.

$$\frac{\partial[H^+]}{\partial \sum[-]} = \left(\frac{\partial \sum[-]}{\partial[H^+]}\right)^{-1}$$

$$\frac{\partial \mathrm{pH}}{\partial \sum[-]} = \left(\frac{\partial \sum[-]}{\partial \mathrm{pH}}\right)^{-1}.$$

In Fig. 2, the effective change in pH, resulting from adding a strong base is depicted as a function of pH. In the absence of a proton buffer, addition of one molecule of a strong base would consume one proton. At pH 8.2, this would be equivalent with a (fictive) pH shift of 55.4 per μmol kg^{-1} increase of the concentration of a strong base. When the marine buffers are present (and at 25 °C, salinity 35 and 1 atm pressure), the change is almost 5 orders of magnitude less. Thus, pH changes with only 1.32 10^{-3} per increase of 1 μmol kg^{-1} of the concentration of the strong base.

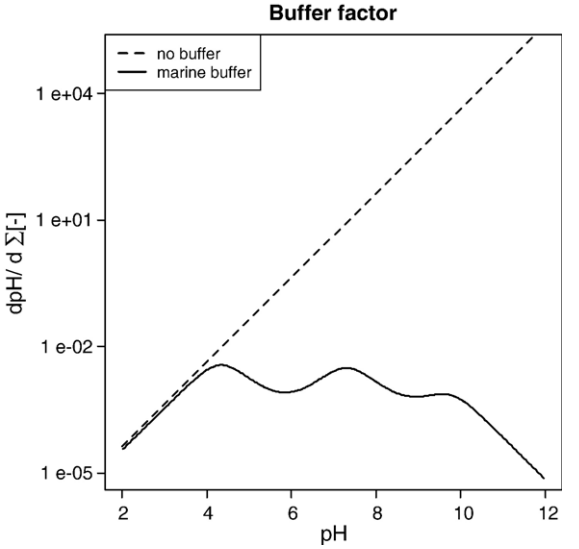

Fig. 2. The buffer factor ($\frac{\partial \mathrm{pH}}{\partial \sum[-]}$), i.e. the change in pH resulting from the addition of a strong base as a function of pH. Dashed line: change in pH in the absence of buffer. See main text for calculations.

4. Non-equilibrium processes

Most of the biogeochemical and physical processes occur at much longer time scales than the acid–base reactions. As these processes change the concentration of acid–base species, this causes readjustment of the chemical equilibria which affects pH. Production of the *uncharged* form of an acid–base that is negatively charged (for example DIC), will release protons to restore the equilibrium, and pH will decrease. In contrast, production of the uncharged form of a component that is positively charged (ammonia at pH < 11), will consume protons and increase pH.

When ion are produced or consumed, it is frequently assumed that this does not cause charging up of the solid phase (particulate organic matter or carbonates) and solutes (e.g. Sikes et al., 1980). In many cases zero charge (electroneutrality) is conserved by the production or consumption of protons or hydroxyl ions (e.g. Brewer and Goldman, 1976) or other acid–base species from Table 2. This exchange of one ion by another ion keeps the concentration of excess negative charge constant; this is formalised by the subscript "[−]=ct".

In some cases, a charged ion that does *not* play part in the acid–base reactions of Table 2 is exchanged to maintain electroneutrality. For instance uptake of Ca^{2+} balances consumption of a carbonate ion in case of carbonate production; Fe^{2+} balances proton exchange during iron oxidation and reduction. Finally, there also exist cases where the electroneutrality assumption is plainly violated, i.e. the total charge of solids and liquids is altered, e.g. during adsorption of ions to solid surfaces. In both of these cases the concentration of excess negative charge changes.

Because of the electroneutrality and equilibrium assumption, the effect on pH is the same, regardless of the exact species of one acid base component whose concentration is altered by the biogeochemical or physical process (e.g. Copin Montégut and Copin Montégut, 1999). This is depicted for the uptake of dissolved inorganic carbon ($\sum CO_2$) in Fig. 3. When CO_2 is taken up, e.g. during photosynthesis, it is continuously replenished from the bicarbonate pool (chemical reaction 1a, Table 2), thereby consuming protons (Fig. 3A). This causes readjustment of the acid–base reaction pairs (Table 2) and increases pH. In contrast, some algae take up bicarbonate rather than CO_2. In this case, either a proton will be consumed (Fig. 3B) or a hydroxyl ion (OH^-) released (Fig. 3C) to keep the algae electroneutral. These changes in proton or hydroxyl ion concentrations also cause readjustment of the equilibria and similar increase in pH.

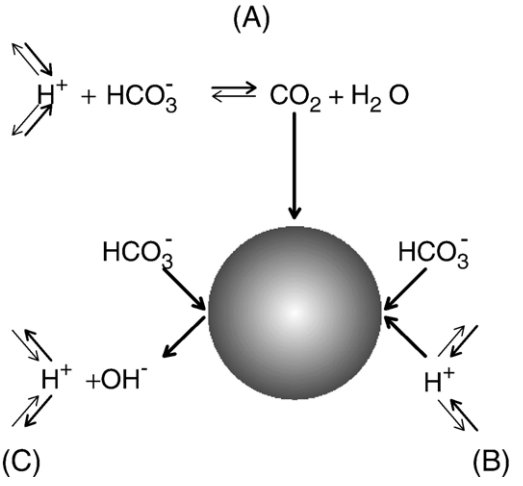

Fig. 3. Schematic representation of DIC uptake whilst conserving the electroneutrality of the solution. A. Uptake of (uncharged) CO_2. B. Uptake or HCO_3^-, negative charge balanced by uptake of H^+. C. Uptake or HCO_3^-, negative charge balanced by release of OH^-.

4.1. The impact of acid–base species on pH

The buffer factor ($\frac{\partial pH}{\partial \Sigma[-]}$, paragraph 3.5) calculates the effect on pH by the addition of a strong base (e.g. NaOH), which changes the concentration of excess negative charge.

In contrast, when during consumption or production of an acid–base species, electroneutrality is maintained by the uptake or release of another acid–base species, the concentration or excess negative charge remains constant and the effect on pH is *reversed*.

We can calculate the effect of any change of an acid–base species ($\sum X$) on pH, assuming that excess negative charge (−) and all other acid–base lump sums (…) remains constant. It is estimated as the rate of change of pH per unit of constituent:

$$\left.\frac{\partial pH}{\partial \Sigma X}\right|_{[-,\ldots]=ct} = -\frac{\partial pH}{\partial \Sigma[-]} \cdot \frac{\partial \Sigma[-]}{\partial \Sigma X}.$$

The term $\frac{\partial \Sigma[-]}{\partial \Sigma X}$ is simply the negative of the mean charge ($\bar{X}^*$) of the species, e.g.

$$\left.\frac{\partial \sum[-]}{\partial \Sigma CO_2}\right|_{[-,\ldots]=ct} = \frac{\partial [HCO_3^-]}{\partial \Sigma CO_2} + 2\frac{\partial [CO_3^{2-}]}{\partial \Sigma CO_2} = \frac{[HCO_3^-] + 2[CO_3^{2-}]}{\Sigma CO_2} = -\overline{CO_2}^*$$

such that:

$$\left.\frac{\partial pH}{\partial \Sigma X}\right|_{[-,\ldots]=ct} = \frac{\partial pH}{\partial \Sigma[-]} \cdot \bar{X}^* \qquad (1)$$

Thus, assuming equilibrium and that electroneutrality is maintained by uptake or release of another acid–base species, the effect of production of an acid–base species ($\sum X$) on pH is simply the product of the single-charge effect on pH (the buffer factor $\frac{\partial pH}{\partial \Sigma[-]}$) and the mean charge of the species ($\bar{X}^*$). For instance, at the reference conditions, production of 1 μmol kg^{-1} DIC will alter the pH by $1.32\times10^{-3}\cdot(-1.12)=-1.48\times10^{-3}$ units.

In order to test whether our derivation is correct, we also estimated numerically, i.e. by perturbation, the changes on pH induced by each species (symbols), and compared this to the predictions (solid line) as derived using the above formula (Fig. 4). The equality (to round off precision) of both estimates demonstrates the correctness of our mathematical derivation. The higher the mean charge of a species, the more its production or consumption affects the pH. ΣCO_2, ΣNO_3 and ΣS are dominated by the univalent anion, whilst ΣPO_4 and ΣSO_4 are predominantly in the form of the bivalent anion. Thus, the release of these latter species will produce about twice as many protons as compared to the former species; all will decrease pH. Silicate is virtually uncharged at pH 8.2, therefore addition or removal of silicate hardly affects pH. Production of ammonium will be accompanied with consumption of protons and increase in pH (Fig. 4).

4.2. Calculating process effects on pH

With the formula (1) derived above, the effect of all single biogeochemical processes on pH can now simply

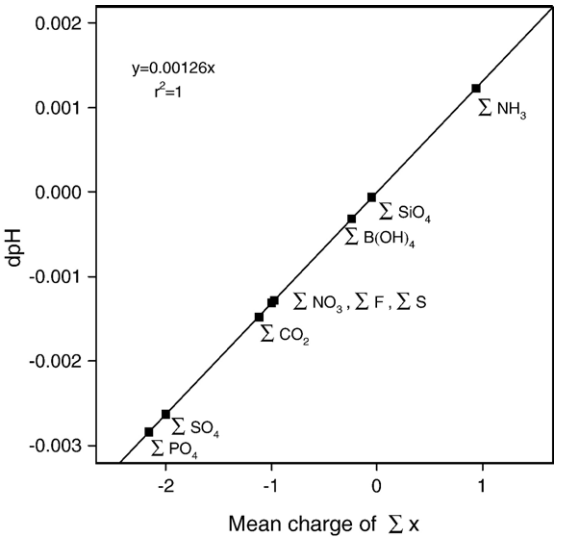

Fig. 4. Effect of changing the concentrations of reactive species ΣX on pH and at pH 8.2, 25 °C, salinity 35, 1 atm, and assuming conservation of electroneutrality (Σ[−]=ct).

be estimated as the sum of the effects of all constituents that are exchanged. The procedure is relatively straightforward in case electroneutrality is maintained by uptake or release of another acid–base species (i.e. the excess negative charge $\Sigma[-]$ is conserved). However, special care needs to be taken when this condition is violated. We give several examples, exemplifying the calculations.

1. The nitrification is one example where the excess negative charge is conserved. The process can be written as follows (using uncharged species):

   $$NH_3 + 2O_2 \Rightarrow HNO_3 + H_2O$$

   The change in pH, for one mole of ammonium oxidised takes into account the charges exchanged by nitrate, and ammonium and the subsequent buffering:

   $$\mathrm{dpH}|_{\mathrm{NH3\_nitrif}} = \frac{\partial \mathrm{pH}}{\partial \Sigma \mathrm{NO_3}} \cdot \mathrm{d}\sum \mathrm{NO_3}|_{\mathrm{nitrif}} + \frac{\partial \mathrm{pH}}{\partial \sum \mathrm{NH_3}} \times \mathrm{d}\sum \mathrm{NH_3}|_{\mathrm{nitrif}}$$

   $$\mathrm{dpH}|_{\mathrm{NH3\_nitrif}} = \frac{\partial \mathrm{pH}}{\partial \Sigma[-]} \cdot (\overline{\mathrm{NO_3^*}} - \overline{\mathrm{NH_x^*}})$$

   As $\frac{\partial \mathrm{pH}}{\partial \Sigma[-]}$ is a positive quantity (Fig. 2), the nitrification decreases pH both by the consumption of ammonium (positively charged at pH < 11) and by the production of nitrate (negatively charged). At the reference conditions, the mean charge of nitrate and ammonium is −1 and +0.937 respectively (Table 1), thus the change in pH per mole of N oxidised is $1.32\times10^{-3}\cdot(-1.937) = -2.55\times10^{-3}$.
2. Electroneutrality is maintained by exchanging species other than the acid–base species from Table 2. Thus, the excess negative charge is altered and the effect of this change on pH also has to be taken into account. Examples are calcification, and iron and manganese reduction, where electroneutrality is maintained by Ca^{2+}, Fe^{2+}or Mn^{2+}.
   - During the production of calcium carbonate, the electroneutrality in the solution and in the carbonate mineral are maintained by the uptake of Ca^{2+} rather than via exchanging protons or OH^-.

     $$Ca^{2+} + CO_3^{2-} \Rightarrow CaCO_3$$

     The effect on pH is then the sum of the effect of consumption of two moles of excess negative charge ($\Sigma[-]$), via bivalent carbonate, and of one mole of DIC.

     $$\mathrm{dpH}|_{\mathrm{calcification}} = -2 \cdot \frac{\partial \mathrm{pH}}{\partial \Sigma[-]} + \frac{\partial \mathrm{pH}}{\partial \Sigma[-]} \cdot (-\overline{\mathrm{CO_2^*}}).$$

     Under natural pH, where the mean charge of DIC is about −1, the effect will be to decrease pH. At very high pH, where the mean charge of DIC is about −2, the pH will be virtually unaltered.
   - During iron reduction, four moles of Fe^{2+} are formed per organic molecule mineralised, and this is compensated by the uptake of 8 moles of protons. As protons contribute negatively to total charge, this is consistent with the production of 8 moles of excess negative charge. The effect of this is added to the charge produced by one mole of DIC, and the production of ammonium and phosphates.
     The effect on pH, per mole of carbon mineralised is

     $$\mathrm{dpH}|_{\mathrm{Fe-reduction}} = 8 \cdot \frac{\partial \mathrm{pH}}{\partial \Sigma[-]} + \frac{\partial \mathrm{pH}}{\partial \Sigma[-]} \times (\overline{\mathrm{CO_2^*}} + \gamma^N \overline{\mathrm{NH_x^*}} + \gamma^P \overline{\mathrm{PO_4^*}})$$

     and where γ^N and γ^P are the N:C and P:C molar ratio of organic matter respectively.
3. In the third example, electroneutrality is plainly violated, e.g. the solid phase charges up.
   - During adsorption of ammonium (NH_4^+), both the excess negative charge and ammonium concentration are affected and the pH change will be:

     $$\Delta\mathrm{pH}|_{\mathrm{adsorption}} = \frac{\partial \mathrm{pH}}{\partial \Sigma[-]} \cdot 1 - \frac{\partial \mathrm{pH}}{\partial \Sigma[-]} \overline{\mathrm{NH_x^*}}$$

     where the '+1' comes from the fact that ammonium negatively contributes to excess negative charge.

4.3. Description of processes considered

Effects of several biogeochemical and physical processes on excess negative charge ($\sum[-]$), on total alkalinity (TA), and pH (the latter estimated at reference conditions, at pH 8.2) are in Table 3.

The decomposition of organic matter (Froelich et al., 1979) includes aerobic respiration (Eq. (1)), denitrification (Eqs. (2) and (3)), iron- (Eq. (4)) and manganese oxide reduction (Eq. (5)), sulphate reduction (Eq. (6))

Table 3
Biogeochemical and physical processes and the impact on excess negative charge ($\Delta\sum[-]$), on total alkalinity (ΔTA) and on pH (dpH)

	Primary redox reactions (1–7)	$\Delta\Sigma[-]$	ΔTA	dpH	pH∞
1	$(CH_2O)(NH_3)_{\gamma N}(PO_4)_{\gamma P} + O_2 \Rightarrow \mathbf{CO_2} + \gamma^N\mathbf{NH_3} + \gamma^P\mathbf{H_3PO_4} + H_2O$	0	$\gamma^N - \gamma^P$	-1.32×10^{-3}	5.18
2	$(CH_2O)(NH_3)_{\gamma N}(PO_4)_{\gamma P} + 0.8\mathbf{HNO_3} \Rightarrow \mathbf{CO_2} + \gamma^N\mathbf{NH_3} + \gamma^P\mathbf{H_3PO_4} + 0.4N_2 + 1.4H_2O$	0	$0.8+\gamma^N-\gamma^P$	-0.26×10^{-3}	7.04
3	$(CH_2O)(NH_3)_{\gamma N}(PO_4)_{\gamma P} + (0.8+0.6\gamma^N)\mathbf{HNO_3} \Rightarrow \mathbf{CO_2} + \gamma^P\mathbf{H_3PO_4} + [0.4+0.8\gamma^N]N_2 + [1.4+1.8\gamma^N]H_2O$	0	$0.8+0.6\gamma^N-\gamma^P$	-0.33×10^{-3}	6.78
4	$(CH_2O)(NH_3)_{\gamma N}(PO_4)_{\gamma P} + 2Fe_2O_3 + 8\mathbf{H^+} \Rightarrow \mathbf{CO_2} + \gamma^N\mathbf{NH_3} + \gamma^P\mathbf{H_3PO_4} + 5H_2O + 4Fe^{2+}$	8	$\gamma^N-\gamma^P+8$	9.2×10^{-3}	+
5	$(CH_2O)(NH_3)_{\gamma N}(PO_4)_{\gamma P} + 2MnO_2 + 4\mathbf{H^+} \Rightarrow \mathbf{CO_2} + \gamma^N\mathbf{NH_3} + \gamma^P\mathbf{H_3PO_4} + 3H_2O + 2Mn^{2+}$	4	$\gamma^N-\gamma^P+4$	3.94×10^{-3}	+
6	$(CH_2O)(NH_3)_{\gamma N}(PO_4)_{\gamma P} + 0.5\mathbf{H_2SO_4} \Rightarrow \mathbf{CO_2} + \gamma^N\mathbf{NH_3} + \gamma^P\mathbf{H_3PO_4} + H_2O + 0.5\mathbf{H_2S}$	0	$\gamma^N-\gamma^P+1$	-0.64×10^{-3}	6.72
7	$(CH_2O)(NH_3)_{\gamma N}(PO_4)_{\gamma P} \Rightarrow 0.5\mathbf{CO_2} + \gamma^N\mathbf{NH_3} + \gamma^P\mathbf{H_3PO_4} + 0.5CH_4$	0	$\gamma^N-\gamma^P$	-0.58×10^{-3}	5.56
	Reoxidation reactions (8–19)	$\Delta\Sigma[-]$	ΔTA	dpH	pH∞
8	$\mathbf{NH_3} + 2O_2 \Rightarrow \mathbf{HNO_3} + H_2O$	0	−2	-2.55×10^{-3}	−
9	$\mathbf{NH_3} + \mathbf{HNO_2} \Rightarrow N_2 + 2H_2O$	0	0	8.20×10^{-5}	7.09,+,−
10	$Mn^{2+} + 0.5O_2 + H_2O \Rightarrow MnO_2 + 2\mathbf{H^+}$	−2	−2	-2.63×10^{-3}	−
11	$Fe^{2+} + 0.5O_2 + H_2O \Rightarrow 0.5Fe_2O_3 + 2\mathbf{H^+}$	−2	−2	-2.63×10^{-3}	−
12	$Fe^{2+} + 0.2\mathbf{HNO_3} \Rightarrow Fe(OOH) + N_2 + 2\mathbf{H^+}$	−2	−2.2	-2.37×10^{-3}	−
13	$Fe^{2+} + 0.5MnO_2 + 0.5H_2O \Rightarrow 0.5Fe_2O_3 + 0.5Mn^{2+} + \mathbf{H^+}$	−1	−1	-1.32×10^{-3}	−
14	$\mathbf{H_2S} + 2O_2 \Rightarrow \mathbf{H_2SO_4}$	0	−2	-1.35×10^{-3}	−
15	$CH_4 + 2O_2 \Rightarrow \mathbf{CO_2} + 2H_2O$	0	0	-1.48×10^{-3}	−
16	$CH_4 + \mathbf{H_2SO_4} \Rightarrow \mathbf{H_2S} + \mathbf{CO_2} + 2H_2O$	0	2	-0.13×10^{-3}	7.88
17	$FeS + 2.25O_2 + H_2O \Rightarrow 0.5Fe_2O_3 + \mathbf{H_2SO_4}$	0	−2	-2.63×10^{-3}	−
18	$FeS + 4MnO_2 + 10\mathbf{H^+} \Rightarrow 4Mn^{2+} + \mathbf{H_2SO_4} + Fe^{2+} + 4H_2O$	10	8	10.52×10^{-3}	+
19	$FeS + 2Fe(OH)_3 + 6\mathbf{H^+} \Rightarrow 3Fe^{2+} + S^0$	6	6	7.89×10^{-3}	+

	Precipitation, other secondary reactions (20–27)	ΔΣ[−]	ΔTA	dpH	pH∞
20	$FeOOH + 1.5\mathbf{H_2S} \Rightarrow FeS + 2H_2O + 0.5S^0$	0	0	1.92×10^{-3}	+
21	$Fe^{2+} + \mathbf{H_2S} \Rightarrow FeS + 2\mathbf{H}^+$	−2	−2	-1.35×10^{-3}	−
22	$FeS + \mathbf{H_2S} \Rightarrow FeS_2 + H_2$	0	0	1.28×10^{-3}	+
23	$Mn^{2+} + \mathbf{CO_3^{2-}} \Rightarrow MnCO_3$	−2	−2	-1.15×10^{-3}	−
24	$Fe^{2+} + \mathbf{CO_3^{2-}} \Rightarrow FeCO_3$	−2	−2	$-1.15\ 10^{-3}$	−
25	$Ca^{2+} + \mathbf{H_2SO_4} + 2H_2O \Rightarrow CaSO_4.2H_2O + 2\mathbf{H}^+$	−2	0	0.0	−
26	$\mathbf{H_2S} + 2Fe(OH)_3 + 4\mathbf{H}^+ \Rightarrow 2Fe^{2+} + S^0 + 6H_2O$	4	4	6.54×10^{-3}	+
27	$\mathbf{H_2S} + MnO_2 + 2\mathbf{H}^+ \Rightarrow Mn^{2+} + S^{0+}2H_2O$	2	2	3.91×10^{-3}	+
	Adsorption, air–sea exchange (28–31)	ΔΣ[−]	ΔTA	dpH	pH∞
28	$\mathbf{H}^+ \Rightarrow H^+_{\equiv}$	1	1	1.32×10^{-3}	+
29	$\mathbf{CO_2} \Rightarrow CO_2(air)$	0	0	1.48×10^{-3}	+
30	$NH_3 \Rightarrow NH_3(air)$	0	−1	-1.23×10^{-3}	−
31	$\mathbf{NH_4^+} \Rightarrow NH_4^+\equiv$	1	0	0.08×10^{-3}	+
	Primary production, calcification,calcite dissolution (32–35)	ΔΣ[−]	ΔTA	dpH	pH∞
32	$\mathbf{CO_2} + \gamma^N\mathbf{NH_3} + \gamma^P\mathbf{H_3PO_4} + H_2O \Rightarrow (CH_2O)(NH_3)_{\gamma N}(PO_4)_{\gamma P} + O_2$	0	$-\gamma^N+\gamma^P$	1.32×10^{-3}	5.18,+,−
33	$\mathbf{CO_2} + \gamma^N\mathbf{HNO_3} + \gamma^P\mathbf{H_3PO_4} + (1+\gamma^N)H_2O \Rightarrow (CH_2O)(NH_3)_{\gamma N}(PO_4)_{\gamma P} + (1+2\gamma^N)O_2$	0	$\gamma^N+\gamma^P$	1.70×10^{-3}	+
34	$\mathbf{CO_3^{2-}} + Ca^{2+} \Rightarrow CaCO_3$	−2	−2	-1.15×10^{-3}	−
35	$CaCO_3 \Rightarrow \mathbf{CO_3^{2-}} + Ca^{2+}$	2	2	1.15×10^{-3}	+

pH∞: the equilibrium pH value; "+": very high pH, "−": very low pH, "+,−": either very low or very high pH (unstable point of zero pH change). See text for more explanation. The effect on pH was calculated for a pH 8.2 (free scale), temperature 25 °C, salinity 35 and pressure 1 atm, using Redfield stoichiometry ($\gamma^N=0.156$; $\gamma^P=0.0094$), and environmental concentrations as in Table 1. In bold are acid–base species.

and methanogenesis (Eq. (7)). Calculations assume Redfield stoichiometry of organic matter.

During organic matter mineralization reduced substances are formed that can subsequently be reoxidised, absorbed or precipitated (e.g. Boudreau, 1996; Van Cappellen and Wang, 1996; Soetaert et al., 1996). Ammonium is reoxidised either by oxygen (nitrification, Eq. (8)) or by nitrite (Eq. (9), the ANAMMOX reaction). Manganese is reoxidised only with oxygen (Eq. (10)), whilst reduced iron may be reoxidised by oxygen (Eq. (11)), nitrate (Eq. (12)) or manganese (hydr)oxides (Eq. (13)). The oxic sulphide and methane reoxidation (Eqs. (14) and (15)), the anoxic oxidation of methane with sulphate (AOM, Eq. 16) and finally the dissolution of the authigenic iron sulphide mineral using oxygen (Eq. 17), or manganese (Eq. 18) or iron oxides (Eq. 19) are also considered.

Precipitation reactions involving acid–base components and that are important mainly in sediments are the precipitation of iron sulphide, using either iron hydroxide (Eq. (20)) or reduced iron (Eq. (21)) as a source and up to pyrite formation (Eq. (22)). Other precipitation reactions are the formation of authigenic carbonate (Eqs. (23) and (24)) and gypsum (hydrated calcium sulphate, Eq. (25)). Dissolved sulphide reacts with iron and manganese oxides resulting in their dissolution and formation of zerovalent sulphur (Eqs. (26) and (27)).

The physical processes described are: proton adsorption on solid surfaces (Eq. (28)), evasion of carbon dioxide and ammonia to the atmosphere (Eqs. (29) and (30)), and adsorption of ammonium to solid surfaces (Eq. (31)).

Finally, we distinguish primary production based on ammonium ((Eq. (32)) or nitrate (Eq. (33)) as a nitrogen source and also include calcium carbonate production (Eq. (34)) and dissolution (Eq. (35)).

5. General response pattern

The effects on pH as a function of pH [2–12] and for all single biogeochemical and physical processes in Table 3 are depicted in Figs. 5–9. They are estimated as the change in pH, per unit of substance x altered by the process, and denoted by dpH. The *unit of substance* x that we refer to can be deduced from Table 3, e.g. for mineralization rates, x is 1 mmol m^{-3} organic matter. These calculations are highly idealised. As they assume that the biogeochemical or physical processes occur in isolation, they are not really intended to reflect natural conditions, in which several processes occur simultaneously and where the effect of one process may trigger the onset of another that annihilates or even reverses the original effect. Note also that, although we calculate the effect of these processes over the pH range of [2–12], this does not mean that all the process actually can take place under these conditions. It is not unlikely that, at extreme pH values, changes in membrane permeability and conductance of organisms, or reductions in the activity of an enzyme involved in some critical pathway, or changes in the solubility of certain elements render the occurrence of the process impossible.

The effect of processes on pH changes with the pH. This is because both the chemical buffer factor (Fig. 2) and the charges of the acid–base components (Fig. 1B) change with pH. In several cases, the process effect on pH is consistently positive or negative over the entire pH range. In other cases, the pH change crosses the 0 axis, and at this pH the rate of change of pH is zero. As is clear from formula (1) this occurs when the net total charge exchanged is 0. The pH at which the rate of change of pH becomes 0 is denoted the 'point of zero pH change' of that process. Depending on the process, pH will either converge to or diverge from such point of zero change. In total, four different response modes can be distinguished (Fig. 5).

(1) Many processes, such as metal oxide reduction, carbonate dissolution, CO_2 evasion to the atmosphere, ammonium and proton adsorption, and nitrate assimilation consistently increase pH across the entire pH range [2–12]. When run infinitely, these processes would converge to very high pH values (Fig. 5A).
(2) Other processes decrease pH across the entire pH range. These include most re-oxidation reactions, calcification, CO_2 invasion from and ammonium release to the air. When run infinitely, these processes would converge to very low pH values (Fig. 5B).
(3) In case the pH change crosses the 0 axis and if it is positive (i.e. pH increases) at pH lower than the point of zero change, and negative at higher pH, then this point of zero pH change is a point of attraction. This means that, all other things remaining equal, the pH will evolve until this point of zero pH change is attained. Once the point of zero change is reached, it will stay there, even if the process continues afterwards. Thus this point is stable. This is the case for most mineralization processes (except metal reduction), and for the anaerobic oxidation of methane (AOM). (Fig. 5C).

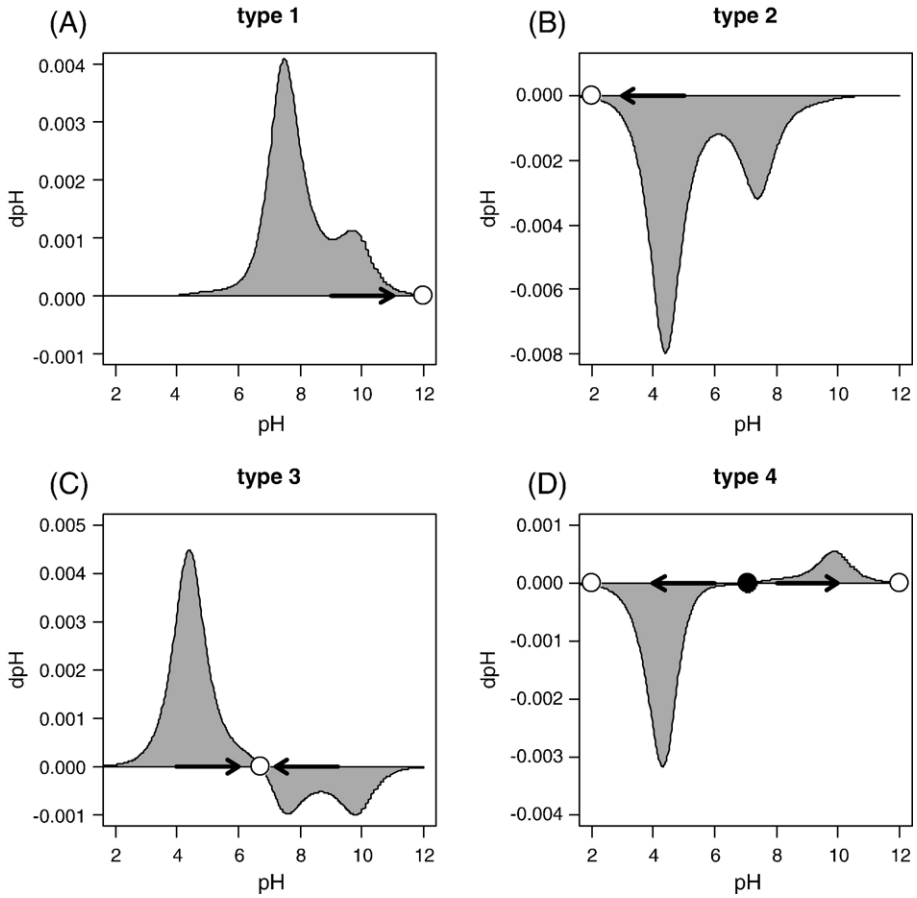

Fig. 5. Patterns of process effects on pH as a function of pH. A. Type 1: monotonic increase of pH. B. Type 2: monotonic reduction of pH. C. Type 3: converging to a stable point of zero pH change. D Type 4: diverging from point of zero pH change. Open circles: pH to which the system evolves (stable point of zero pH change). Closed circle: pH from which system diverges (unstable point of zero change).

(4) In contrast, if the rate of change of pH is positive above and negative below the point of zero pH change, then pH will drift away from that point, and in directions that are determined by the initial pH. If the initial pH is higher than the point of zero pH change, the process will converge to very high pH, if initial pH is smaller than the point of zero pH change, it will converge to very low pH. Thus this point is unstable, as small perturbations will cause divergence. This is the case for ammonium assimilation and for the ANAMMOX reaction (Fig. 5D).

5.1. Effect of mineralization processes

At normal pH values (~8), oxic organic matter respiration liberates carbon dioxide, whose dissociation (Table 2, Eq. (1)) produces protons and lowers the pH. At pH>5.2, this acidification by far overrules the counterbalancing effect due to the production of ammonium. Below pH 5.2, the small negative charge produced by inorganic carbon is surpassed by the positive charge (ammonium) formed and the effect of oxic mineralization on pH is reversed (Fig. 6A). The behaviour is quite similar in methanogenesis although the impact on pH is not as large (Fig. 6D), as only half the amount of dissolved inorganic carbon is produced. Also, the point of zero pH change of methanogenesis (5.6) is slightly above the one from the oxic mineralization (5.2; Table 3.7).

During denitrification (Fig. 6B) and sulphate reduction (Fig. 6D), negatively charged substances are not only produced (ΣCO_2), but also consumed (ΣNO_3, ΣSO_4). Because of that and at pH ~ 8, these processes

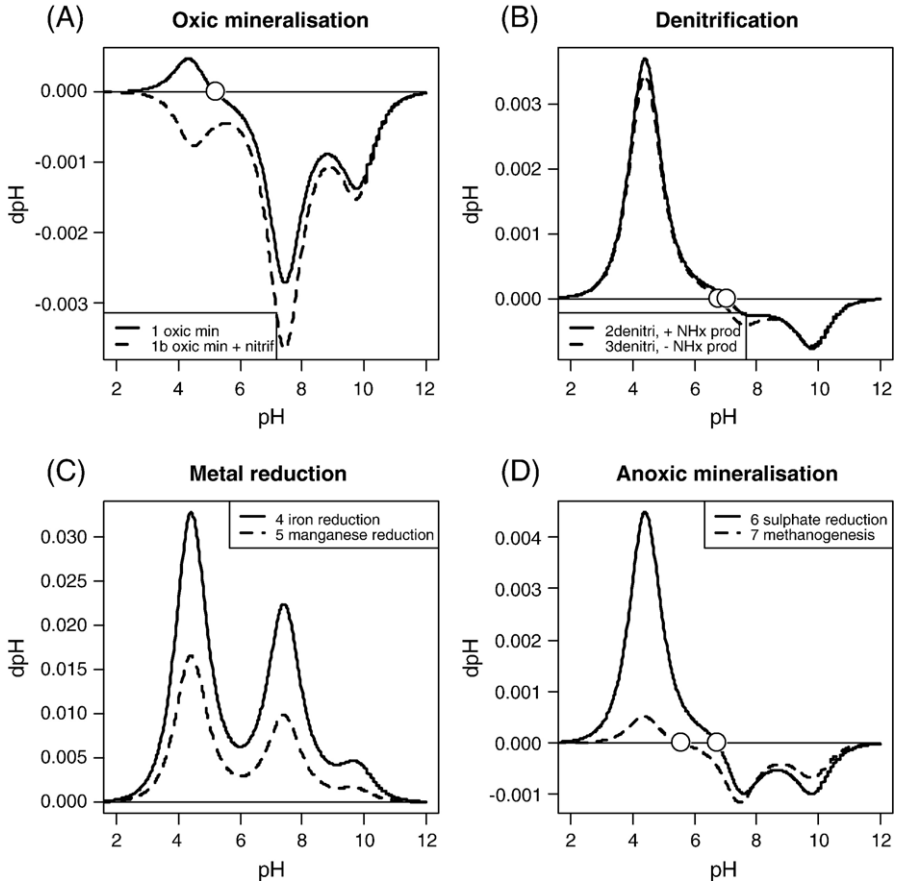

Fig. 6. Effect of mineralization processes on pH (dpH), expressed per unit of carbon mineralised. Stable points of zero pH change denoted with open circles. Numbers refer to equations in Table 3.

have less effect than oxic mineralisation. However, at low pH values, where the (ΣCO_2), has lost its charge, the consumption of negatively charged substances (nitrate, sulphate) reinforces the production of the positively charged ammonium, hence the large pH increasing effect under these conditions (Fig. 6B, D). Another consequence of this is that the point of zero pH change is reached at higher levels (6.8–7.0 for denitrification and 6.7 for sulphate reduction; Table 3) compared to oxic mineralization.

Protons are consumed, and pH rises, while Mn and Fe (hydr)oxides are reduced (Fig. 6C). The iron reduction has twice the impact of the manganese reduction. At pH ~ 8, their effect is 3 to 7 times more pronounced and reversed compared to the oxic mineralisation. As the proton consumption by far exceeds the effect of production of DIC and the lesser species, these processes have a consistent impact on pH over the entire pH range [2–12].

5.2. Effect of reoxidation processes

Except for the anaerobic ammonium oxidation (ANAMMOX) and the anaerobic oxidation of methane (AOM) and FeS, all reoxidation reactions monotonically decrease pH. Reoxidation of Mn^{2+}, Fe^{2+} and FeS by oxygen shares the production of equal amounts of protons (the latter by dissociation of sulphate) and therefore exhibits the same response (Fig. 7A). Nitrification reduces the pH, in a similar extent as the reoxidation of these metals, except for pH > 8, where ammonium looses its charge (Fig. 7A). The aerobic reoxidation of sulphide and methane has lower effect on pH (Fig. 7B). In case of iron reoxidation, the impact on pH is largest when oxygen is used as an oxidant, followed by the oxidation based on nitrate and finally manganese oxides (Table 3). In the ANAMMOX reaction, both ammonium and nitrite are consumed in a ratio of 1:1. At low pH (<4) where ammonium is fully

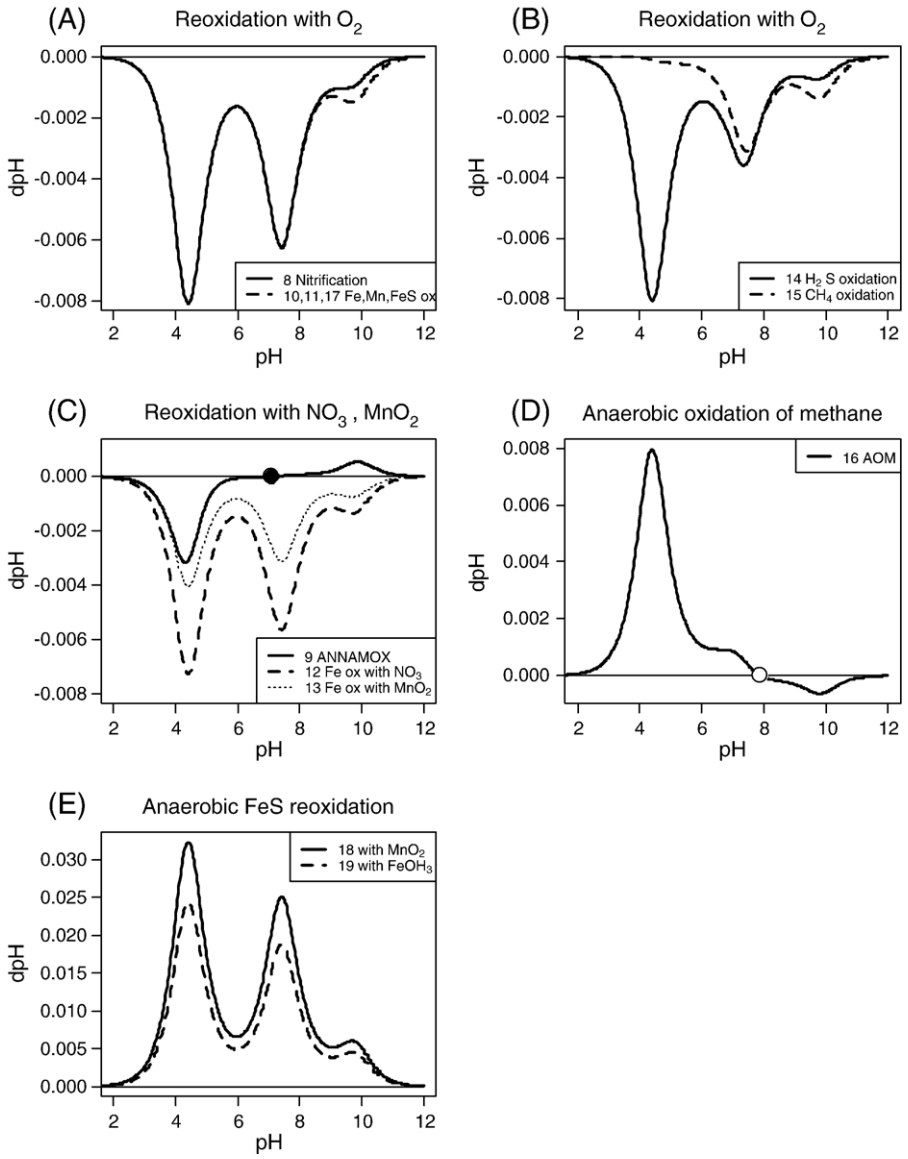

Fig. 7. Effect of reoxidation processes on pH, expressed per unit of substance reoxidised. Stable points of zero pH change denoted with open circles. Unstable points of zero pH change denoted with closed circle. Numbers refer to equations in Table 3.

protonated and nitrite is mainly uncharged, the uptake of ammonium releases protons and decreases pH. At high pH, ammonia has lost its charge, but the removal of fully charged nitrite provokes proton consumption and increases pH. At pH of ~7.1, both nitrite and ammonium have equal charge, and the reaction does not affect pH (Fig. 7C; Table 3.9). However, small perturbations will lead to divergence from this pH (the point of zero pH change is unstable). During anaerobic methane oxidation (AOM), the consumption of sulphate, increasing pH, competes with the production of sulphide and dissolved inorganic carbon, which both tend to decrease pH. As the mean charges of DIC and sulphide increase with higher pH, whilst sulphate remains fully dissociated, the effects of the former become more important as pH increases. At pH 7.9, the mean charge consumed by sulphate (−2) is exactly balanced by the charges of the DIC (−1.053) and sulphide (−0.947) produced (Fig. 7D; Table 3.16). The reoxidation of iron sulphide by manganese oxides and iron hydroxides is accompanied by large quantities of protons released

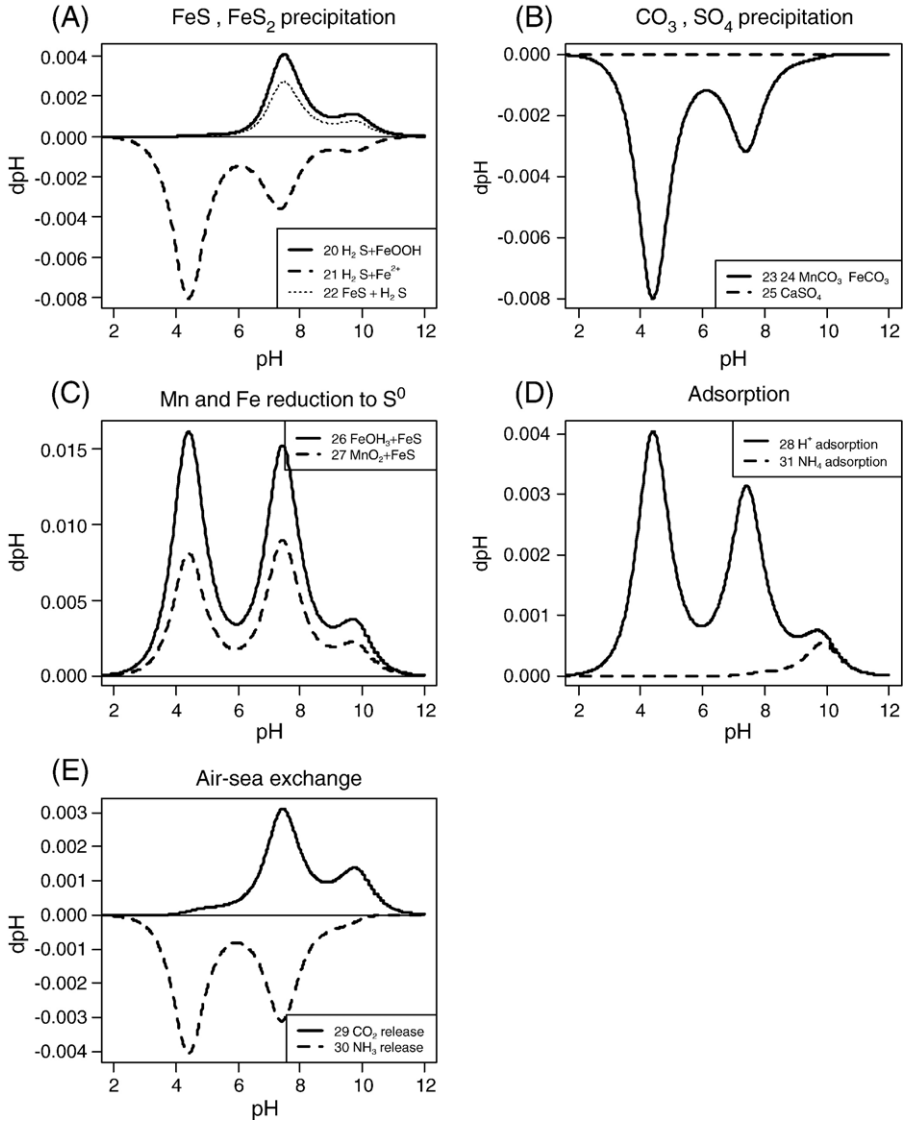

Fig. 8. Effect of adsorption, secondary redox processes, proton addition and CO_2 input from atmosphere, on pH. Numbers refer to equations in Table 3.

and thus monotonically increase pH (Fig. 7E). Note the comparatively large impact of these processes on pH, of similar magnitude as the iron reduction (Table 3).

5.3. Precipitation, dissimilatory reduction, physical processes

FeS can be formed either via dissolution of ferric hydroxide with sulphide (Eq. (20)) or using Fe^{2+} (Eq. (21)) (Fig. 8A). In the former case pH will increase, whilst consumption of Fe^{2+} will decrease pH. The consecutive reduction, with sulphide, of FeS to pyrite (Eq. (22)) increases pH. Thus the effect on pH will be most pronounced when iron hydroxides are the source of iron to produce FeS and its further reaction to pyrite (e.g. Boudreau and Canfield, 1993).

Dissolved metals (Fe^{2+}, Mn^{2+}), produced by metal oxide reduction can also precipitate as a reduced authigenic carbonate mineral (Eqs. (23) and (24)). The effect of these reactions is to monotonically decrease pH (Fig. 8B). The formation of gypsum (Eq. (25)) has no effect on pH, except at very low pH values (Fig. 8B). This is because the positive charge of Ca^{2+} is exactly

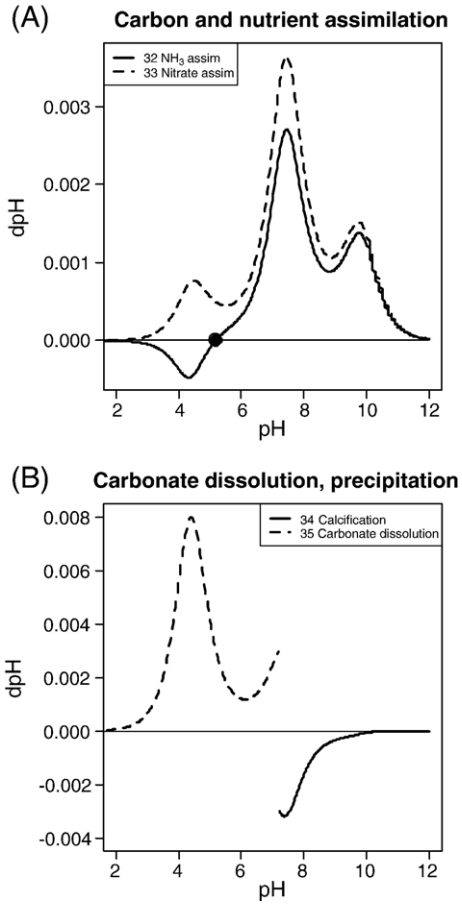

Fig. 9. Effect of primary production and calcification, and calcite dissolution processes on pH. Unstable points of zero pH change denoted with closed circle. Numbers refer to equations in Table 3.

matched by the bivalence of sulphate, which is fully dissociated above pH 3.0. This is an example of a process that affects total alkalinity without impacting pH.

Iron and manganese (hydr)oxide reduction with sulphide (Eqs. (26) and (27); Fig. 8C), and producing S^0 increases pH, similar as the assimilatory reduction (Eq. (4), (5)) but the effect is slightly lower.

Surface-active species (NH_4^+, H^+) can be adsorbed to solid surfaces (Fig. 8D). The effect is smaller for ammonium than for protons, as the loss of charge induced by ammonium removal is partly counterbalanced by the protonation of ammonia.

At pH > 7.5, pH increase induced by CO_2 evasion is somewhat higher than the one induced by H^+ removal (Fig. 8D), as the mean charge of DIC is slightly more negative than −1. The effect of CO_2 addition or removal is reduced with decreasing pH, as more and more of the DIC is in the form of the uncharged CO_2 (Fig. 8E). Ammonium release to the air decreases pH. Overall, the effect of this process on pH mirrors proton adsorption, except at pH > 7.3, where ammonium starts loosing its charge.

5.4. Primary production, calcification

By taking up DIC, negatively charged at pH > 4, photosynthesis generally increases the pH. In case the algae grow on nitrate, the uptake of (negatively charged) nitrate will enhance this effect, whilst when growing on ammonium (positively charged at pH < 11), the effect is reduced (Fig. 9A). Below pH 5.2, the effects of ammonium uptake surpass the effects induced by uptake of DIC. Note that the response pattern of nitrate and ammonium assimilation (Fig. 9A) mirrors those of the oxic mineralization with or without nitrification (Fig. 6A). However, whereas the point of zero pH change is stable in case of aerobic respiration, it is unstable in the case of ammonium assimilation.

Calcification is the process whereby Ca^{2+} and carbonate or bicarbonate ions precipitate to form crystals of the calcium carbonate minerals calcite or aragonite. The calcite or aragonite saturation state determines whether calcium carbonate will be formed (>1) or will dissolve (<1). Under the prevailing environmental conditions, the pH at which the calcite or aragonite saturation state is 1 is attained at 7.2 and 7.4 respectively. As calcification consumes excess negative charge as well as DIC, its effect is to lower pH (at pH > 7.2, 7.4). The reverse is true for calcite and aragonite dissolution (Fig. 9B).

6. Discussion

Process effects on the pH–pCO_2 system have traditionally been expressed by simple numbers. For instance, the chemical buffer factor describes pH variation related to input of an inorganic carbon species (Riley and Skirrow, 1975), the homogeneous buffer factor or Revelle factor depicts relative variations of partial CO_2 pressure with total inorganic carbon (Sundquist and Plummer, 1979). Frankignoulle (1994) and Frankignoulle et al. (1994) quantified the effect of carbonate production on pH and pCO_2. In this paper we have re-derived, generalised and extended this approach. We show that process effects on pH can be calculated as the product of (1) the net exchange of charge by consumption and or production of acid–base components and (2) the subsequent buffering of pH variations. It is common knowledge (Stumm and Morgan, 1981; Zeebe and Wolf-Gladrow, 2001) that the acid–base composition of many biogeochemically-

active substances depends on the physicochemical properties of the water, and thus also on pH. Similarly, the buffering capacity of the solution (the ability to absorb or release protons) is highly affected by the free proton concentration. Because of this, the impact of biogeochemical and physical processes on pH or pCO_2 changes with pH (e.g. Frankignoulle et al., 1994). To demonstrate this, we have calculated the effects of single biogeochemical processes along an extensive pH gradient [2–12]. These calculations provide a reference frame against which temporal or spatial changes in pH can be understood qualitatively. In what follows we first discuss what typically shapes pH in water and sediments. As our results emphasize the long-term effects of single processes on pH, they can be used to put into perspective certain findings reported in the literature. We then give two examples that relate to the calcification process, i.e. why it co-occurs with the anaerobic oxidation of methane and what are the environmental consequences of its co-occurrence with photosynthesis.

The water column is usually an oxic environment where changes in pH mainly result from carbon and nitrogen processes (e.g. Zhang, 2000). Organic matter and carbonates are produced in the euphotic zone and, after sinking, remineralise and dissolve at greater depth. As these processes have different effects on pH, typical gradients ensue. Water-column pH is kept into a typical range of (7.3–8.2), mainly by the carbonate cycle: at depth, the dissolution of carbonates (at low pH), increases pH (Table 3 Eq. (35); Fig. 9B) and thus buffers the acidity released by the mineralisation reactions (Table 3 Eq. (1); Fig. 6A). Near the surface carbonate precipitation (Table 3 Eq. (34); Fig. 9B) may reduce the pH increase induced by photosynthesis (Table 3 Eqs. (35) and (36); Fig. 9A). As calcite dissolution occurs at larger depth than organic matter mineralization, a typical pH dip is observed in the zone where most of the mineralization takes place (Millero et al., 1998; Zhang, 2000). This pH minimum is reinforced by the depth separation of nitrate consumption near the surface (increasing pH) and production at depth (decreasing pH, Table 3 Eq. (8); Fig. 7A).

The variety and concentrations of protolytic species such as sulphide, ammonium, phosphates, but also DIC is often much higher in anoxic seawater and sediments than in oxic seawater. Consequently, anoxic seawater and sediments are better buffered against pH variations (not shown). The sequential utilization of electron acceptors by micro-organisms that mineralise the organic matter provokes a characteristic depth zonation of redox conditions in these environments. Due to this biogeochemical complexity, sediment and anoxic basin pH is not only impacted by the carbon and nitrogen cycle, but also by the sulphur, manganese and iron cycle. In sediments, oxic mineralization (Table 3 Eq. (1)) and the oxic reoxidation of reduced substances (ammonium, Fe^{2+}, Mn^{2+}, sulphide and methane, Table 3 Eqs. (8),(10), (11),(14),(15)) all reduce pH (Fig. 7A,B), causing sharp drops in pore water pH below the sediment–water interface. The pH generally reaches its minimum at the oxic–anoxic transition zone (e.g. Revsbech et al., 1983; Archer et al., 1989; Luff et al., 2001; Wenzhofer et al., 2001). Below this, pH often increases due to the combined effects of dissimilatory Fe- and Mn-oxide reduction (e.g. Reimers et al., 1996; Wenzhofer et al., 2001). Indeed, although the importance of Mn and Fe oxides in organic matter mineralization is generally limited (but see Aller, 1990), the relative impact on pH by this process is much higher than any other process (Table 3 Eqs. (4) and (5); Fig. 6C) and the importance of these processes can therefore be deduced from pore-water pH profiles (Reimers et al., 1996). Finally, the sulphur cycle may well have the strongest effect on pH, keeping it in the range of (6.9–8.3) (Ben-Yaakov, 1973); whilst carbonate dissolution and precipitation generally have a lower impact on the pH in sediments (Boudreau and Canfield, 1993).

The interactive effects of production and consumption of multiple species during biogeochemical processes on pH sometimes produce unusual results. Although many processes either consistently increase or lower pH, this is not always the case. For instance, except for Fe and Mn oxide reduction, the mineralization of organic matter may either increase, or decrease pH depending on the pH at which the process takes place. This has been shown before for sulphate reduction under closed and open-system conditions (Boudreau and Canfield, 1993). Here we show that this phenomenon is more general and also applies to the oxic mineralisation (Fig. 6A), denitrification (Fig. 6B), and methanogenesis (Fig. 6D). Ben-Yaakov (1973) demonstrated that, when considering sulphate reduction and ignoring transport, the pH in sediments will converge to a range of (6.9–8.3), the lower pH attained when sulphide accumulates in the sediment, the latter pH when sulphide is removed by precipitation to iron sulphide. This finding is confirmed here (Fig. 6D, 8A), but we show that convergence to one pH value is a general phenomenon for most mineralisation reactions (Fig. 6A,B,D), except for metal reduction. This point of zero pH change is attained when the net charges produced and consumed exactly balance; at 25 °C, salinity 35 and 1 atm pressure

this is in between 5.2 (oxic mineralization) and 7.0 (denitrification).

The anaerobic oxidation of methane (AOM) shows similar behaviour (Table 3 Eq. (16); Fig. 6D). This process occurs in coastal and continental margin sediments, in seeps and in hydrothermal vent sediments, which have an unusual mix of high methane and sulphate concentrations and it is often strongly linked with carbonate production (e.g. Wallmann et al., 1997; Valentine, 2002).

In general, the co-occurrence of AOM and carbonate precipitation is attributed to the fact that the AOM process increases alkalinity (or bicarbonate), which is then consumed by carbonate precipitation (Ritger et al., 1987; Middelburg et al., 1990). The typical way in which the anoxic methane oxidation is written indeed suggests bicarbonate formation:

$$CH_4 + SO_4^{2-} \rightarrow HCO_3^- + HS^- + H_2O.$$

However, this does not explain why the sulphate reduction (Table 3 Eq. (6)) linked to organic matter respiration does not lead to calcification. Typical writing of this process also produces bicarbonate and thus also suggests coupling with calcification:

$$CH_2O + 0.5SO_4^{2-} \rightarrow HCO_3^- + 0.5HS^-.$$

However, in order to link both processes, the long-term effects of sulphate reduction on pH need to be taken into account. When initiated at pH ~ 8, both sulphate reduction and AOM will reduce the pH. However, AOM converges to a pH of 7.9, well above the critical pH above which carbonate precipitation is possible (7.2–7.4). Thus, as calcification lowers pH below 7.8, the AOM will counteract this and tend to increase pH. In contrast, the sulphate mineralization pathway converges to a much lower point of zero pH change (pH 6.7), well below the critical pH for carbonate precipitation. Therefore, unless the process is accompanied by precipitation of sulphides with iron oxides (e.g. Ben-Yaakov, 1973; Coleman and Raiswell, 1995), sulphate reduction will not lead to carbonate production on a scale sufficient to form concretions, as is the case for AOM (Raiswell and Fisher, 2004; Middelburg et al., 1990).

Ammonium assimilation and anaerobic ammonium oxidation (ANAMMOX) either tend to very low or very high pH, depending on initial conditions. The critical pH from which the former process diverges is quite low (~5.2). Although the ANAMMOX process diverges from more realistic pH values (~7.1), at a typical pH of 8, the process has very little effect on pH (around 2 orders of magnitude less than nitrification, Table 3.9). Therefore, this behaviour of these two processes may not have important environmental consequences. However, similar behaviour has been documented in literature for a combination of processes.

In many calcifying organisms, calcification (C) is at least loosely coupled to photosynthesis (P). Both processes consume DIC, but calcification decreases, whilst photosynthesis increases pH. Because of the shift in the chemical equilibria concomitant with the drop in pH, CO_2 is generated rather than consumed during calcification (Wollast et al., 1980), whilst it is consumed by photosynthesis. Due to these antagonistic effects, the net impact of calcifying organisms on the pH–pCO_2 of the environment depends on the calcification:production (C:P) ratio (Crawford and Purdie, 1997). It has been shown both for coccolithophorids (Buitenhuis et al., 2001) and corals (e.g. Gattuso et al., 1999) that, for typical pH values, pCO_2 will be conserved at C:P ratios of about 1.2 or 1.7 when growing on ammonium or nitrate respectively, whilst pCO_2 decreases at lower and increases at higher ratios, and this observation has raised issues as to the impact of these organisms on the CO_2 storage capacity in the ocean. Indeed, the combination of both processes leads to a complex pH response pattern (type 4) that is characterised by the presence of an unstable point of zero pH change, from which the pH will diverge. In case the organisms grow on nitrate, the point of zero pH change is attained at pH 6.8 (C:P 1.0) and 8.1 (C:P 1.5), in case of growth on ammonium, it is attained at 7.8 (C:P 1.0) and 8.4 (C:P 1.5).

Acknowledgements

In the year 2004, Belgium lost two of its strongholds in chemical oceanography, Michel Frankignoulle and Roland Wollast. The paper that we present here was clearly inspired by Frankignoulle's paper in 1994. However, being a biologist (KS) interest for chemical oceanography was mainly aroused by Roland's works and his performance as a coordinator of the OMEX project. This project gave a boost in the career of KS. Two anonymous reviewers, and Bernie Boudreau, are thanked for constructive feedback. The first version of the pH model was created during the last phase of the OMEX project (MAS3-CT96-0056). It was subsequently improved during the ORFOIS project (EVK2-CT2001) and now applied in the framework of the Carbo-Ocean (511176-2) and HERMES project (GOCE-CT-2005-511234-1). This is article number 3933 from the NIOO-CEME, Yerseke.

Appendix A. Derivatives of charges

The derivative of the charge of a univalent species ($a=1$) with respect to [H+]:

$$\frac{dX^*}{d[H^+]} = -\frac{K_X}{([H^+]+K_X)^2}$$

The derivative of the charge of a bivalent species ($a=2$) with respect to [H+] (Park, 1969):

$$\frac{dX^*}{d[H^+]} = \frac{-K_1^2\cdot K_2 - K_1\cdot[H^+]^2 - 4K_1\cdot K_2\cdot[H^+]}{([H^+]\cdot[H^+]+K_1\cdot[H^+]+K_1\cdot K_2)^2}.$$

The derivative of the charge of a trivalent species ($a=3$) with respect to [H+]:

$$\frac{dX^*}{d[H^+]} = \frac{-4K_1^2K_2K_3\cdot[H^+] - K_1^2K_2\cdot[H^+]^2 - 4K_1K_2\cdot[H^+]^3 - K_1\cdot[H^+]^4 - K_1^2K_2^2K_3 - 9K_1K_2K_3\cdot[H^+]^2}{([H^+]^3+[H^+]^2K_1+[H^+]\cdot K_1\cdot K_2+K_1\cdot K_2\cdot K_3)^2}$$

References

Aller, R.C., 1990. Bioturbation and manganese cycling in hemipelagic sediments. Philos. Trans. R. Soc. Lond., A 331, 51–68.

Archer, D., Emerson, S., Reimers, C., 1989. Dissolution of calcite in deep-sea sediments — pH and O_2 microelectrode results. Goechim. Cosmochim. Acta 53, 2831–2845.

Ben-Yaakov, S., 1973. pH buffering of pore waters of recent anoxic marine sediments. Limnol. Oceanogr. 18, 86–94.

Boudreau, B.P., Canfield, D.E., 1993. A comparison between closed- and open-system models for porewater pH and calcite-saturation state. Geochim. Cosmochim. Acta 57, 317–334.

Boudreau, B.P., 1996. A method-of-lines code for carbon and nutrient diagenesis in aquatic sediments. Comput. Geosci. 22, 479–496.

Brewer, P.G., Goldman, J.V., 1976. Alkalinity changes generated by phytoplankton growth. Limnol. Oceanog. 21, 108–117.

Broecker, W.S., Peng, T.H., 1982. Tracers in the Sea. Eldigio Press, Palisades, New York. 690pp.

Bronshteyn, V.K., Chernov, A.A., 1991. Freezing potentials arising on solidification of dilute aqueous solutions of electrolytes. J. Cryst. Growth 112, 129–145.

Buitenhuis, E.T., van der Wal, P., De Baar, H.J.W., 2001. Blooms of *Emiliana huxleyi* are sinks of atmospheric carbon dioxide: a field and mesocosm study derived simulation. Glob. Biogeochem. Cylces 15, 577–587.

Cai, W.-J., Wang, Y., 1998. The chemistry, fluxes and sources of carbon dioxide in the estuarine waters of the Satilla and Altamaha Rivers, Georgia. Limnol. Oceanogr. 43, 657–668.

Cai, W.-J., Wang, Y., Hodson, R., 1998. Acid–base properties of dissolved organic matter in the estuarine waters of Georgia, USA. Geochim. Cosmochim. Acta 62, 473–483.

Coleman, M.L., Raiswell, R., 1995. Source of carbonate and origin of zonation in pyretiferous carbonate concretions — evaluation of a dynamic model. Am. J. Sci. 295, 282–308.

Copin Montégut, C., Copin Montégut, G., 1999. Theoretical considerations about the reactions of calcification in sea water. Mar. Chem. 63, 213–224.

Crawford, D.W., Purdie, D.A., 1997. Increase of pCO_2 during blooms of *Emiliana huxleyi*: theoretical considerations on the asymmetry between acquisition of HCO_3^- and respiration of free CO2. Limnol. Oceanogr. 42, 365–372.

Dickson, A.G., 1981. An exact definition of total alkalinity and a procedure for the estimation of alkalinity and total inorganic carbon from titration data. Deep-Sea Res. 28A, 609–623.

Ferris, F.G., Hallbeck, L., Kennedy, C.B., Pedersen, K., 2004. Geochemistry of acidic Rio Tinto headwaters and role of bacteria in solid phase metal partitioning. Chem. Geol. 212, 291–300.

Follows, M.J., Williams, R.G., Marshall, J.C., 1996. The solubility pump of carbon in the subtropical gyre of the North Atlantic. J. Mar. Res. 54, 605–630.

Frankignoulle, M., 1994. A complete set of buffer factors for acid/base CO_2 system in seawater. J. Mar. Syst. 5, 111–118.

Frankignoulle, M., Canon, C., Gattuso, J.P., 1994. Marine calcification as a source of carbon dioxide: positive feedback of increasing atmospheric CO_2. Limnol. Oceanogr. 39, 458–462.

Froelich, P.N., Klinkhammer, G.P., Bender, M.L., Luedtke, N.A., Heath, G.R., Cullen, D., Dauphin, P., 1979. Early oxidation of organic matter in pelagic sediments of the eastern equatorial Atlantic: suboxic diagenesis. Geochim. Cosmochim. Acta 43, 1075–1090.

Gattuso, J.P., Frankignoulle, M., Smith, S.V., 1999. Measurement of community metabolism and significance in the coral reef CO_2 source–sink debate. Proc. Natl. Acad. Sci. U. S. A. 96, 13017–13022.

Gleitz, M., Rutgers van der Loeff, M.M., Thomas, D.N., Dieckmann, G.S., Millero, F.J., 1995. Comparison of summer and winter inorganic carbon, oxygen and nutrient concentrations in Antarctic sea ice brine. Mar. Chem. 51, 81–91.

Hunter, K.S., Wang, Y., van Cappellen, P., 1998. Kinetic modeling of microbially-driven redox chemistry of subsurface environments: coupling transport, microbial metabolism and geochemistry. J. Hydrol. 209, 53–80.

Jeppesen, E., Sondergaard, M., Jensen, J.P., Mortensen, E., Hansen, A.M., Jorgensen, T., 1998. Cascading trophic interactions from fish to bacteria and nutrients after reduced sewage loading: an 18-year study of a shallow hypertrophic lake. Ecosystems 1, 250–267.

de Lange, G.J., Middelburg, J.J., Van der Weijden, C.H., Catalano, G., Luther, G.W., Hydes, D.J., Woittiez, J.R.W., Klinkhammer, G.P., 1990. Composition of anoxic hypersaline brines in the Tyro and Bannock Basins, eastern Mediterranean. Mar. Chem. 31, 63–88.

Lewis, E., Wallace, D.W.R., 1998. Program developed for CO_2 system calculations. ORNL/CDIA-105. Carbon dioxide information analysis center, Tennessee, USA.

Luff, R., Haeckel, M., Wallmann, K., 2001. Robust and fast FORTRAN and MATLAB libraries to calculate pH distributions in marine sediments. Comput. Geosci. 27, 157–169.

Meysman, F.J.R., Middelburg, J.J., Herman, P.M.J., Heip, C.H.R., 2003. Reactive transport in surface sediments. II. Media: an object-oriented problem-solving environment for early diagenesis. Comput. Geosci. 29 (3), 301–318.

Middelburg, J.J., de Lange, G.J., Kreulen, R., 1990. Dolomite formation in anoxic sediments of Kau Bay, Indonesia. Geology 18, 399–402.

Millero, F.J., 1995. Thermodynamics of the carbon dioxide system in the oceans. Geochim. Cosmochim. Acta 59, 661–677.

Millero, F.J., Degler, E.A., O'Sullivan, D.W., Goyet, C., Eischeid, G., 1998. The carbon dioxide system in the Arabian Sea. Deep-Sea Res. II 45, 2225–2252.

Morris, A.W., Riley, J.P., 1966. The bromide/chlorinity and sulphate/chlorinity ratio in seawater. Deep-Sea Res. 13, 699–706.

Park, P.K., 1969. Oceanic CO_2 system: an evaluation of ten methods of investigation. Limnol. Oceanogr. 14, 179–186.

Press, W.H., Teukolsky, S.A., Vetterling, W.T., Flannery, B.P., 1997. Numerical recipes in FORTRAN 77: the art of scientific computing, 3rd ed. Cambridge University Press, Cambridge.

Raiswell, R., Fisher, Q.J., 2004. Rates of carbonate cementation associated with sulphate reduction in DSDP/ODP sediments: implications for the formation of concretions. Chem. Geol. 211, 71–85.

Reimers, C.E., Rutgenberg, K.C., Canfield, D.E., Christiansen, M.B., Martin, J.B., 1996. Pore water pH and authigenic phases formed in the uppermost sediments of the Santa Barbara Basin. Geochim. Cosmochim. Acta 60, 4037–4057.

Revsbech, N.P., Jørgensen, B.B., Blackburn, T.H., 1983. Micro-electrode studies of the photosynthesis and O_2, H_2S and pH profiles of a microbial mat. Limnol. Oceanogr. 28, 1062–1074.

Riley, J.P., 1965. The occurrence of anomalously high fluoride concentrations in the North Atlantic. Deep-Sea Res. 12, 219–220.

Riley, J.P., Skirrow, G., 1975. 2nd ed. Chemical oceanography, Vol 2. Academic Press, London.

Ritger, S., Carson, B., Suess, E., 1987. Methane-derived authigenic carbonates formed by subduction-induced porewater expulsion along the Oregon/Washington margin. Geol. Soc. Amer. Bull. 98, 147–156.

Schoonen, M.A.A., Barnes, H.L., 1988. An approximation of the 2nd dissociation-constant for H_2S. Geochim. Cosmochim. Acta 52, 649–654.

Sikes, C.S., Roer, R.D., Wilbur, K.M., 1980. Photosynthesis and coccolith formation: inorganic carbon sources and net inorganic reaction of deposition. Limnol. Oceanogr. 25, 248–261.

Smith, S.V., Key, G.S., 1975. Carbon dioxide and metabolism in marine environments. Limnol. Oceanogr. 20, 493–495.

Soetaert, K., deClippele, V., Herman, P., 2002. Femme, a flexible environment for mathematically modelling the environment. Ecol. Modell. 151, 177–193.

Soetaert, K., Herman, P.M.J., Middelburg, J., 1996. A model of early diagenetic processes from the shelf to abyssal depths. Geochim. Cosmochim. Acta 60, 1019–1040.

Stumm, W., Morgan, J.J., 1981. Aquatic Chemistry, 2nd Ed. John Wiley and sons, New York, p. 780.

Sundquist, E.T., Plummer, L.N., 1979. Carbon dioxide in the ocean surface: the homogeneous buffer factor. Science 204, 1203–1205.

Taylor, A.H., Watson, A.J., Robertson, J.E., 1992. The influence of the spring phytoplankton bloom on carbon dioxide and oxygen concentrations in the surface waters of the northeast Atlantic during 1989. Deep-Sea Res. 39, 137–152.

Valentine, D.L., 2002. Biogeochemistry and microbial ecology of methane oxidation in anoxic environments: a review. Antonie van Leeuwenhoek 81, 271–282.

Van Cappellen, P., Wang, Y., 1996. Cycling of iron and manganese in surface sediments: a general theory for the coupled transport and reaction of carbon, oxygen, nitrogen, sulfur, iron and manganese. Am. J. Sci. 296, 197–243.

Wallmann, K., Linke, P., Suess, E., Bohrmann, G., Sahling, H., Schluter, M., Dahlmann, A., Lammers, S., Greinert, J., von Mirbach, N., 1997. Quantifying fluid flow, solute mixing and biogeochemical turnover at cold vents of the eastern Aleutian subduction zone. Geochim. Cosmochim. Acta 61, 5209–5219.

Ware, J.R., Smith, S.V., Reaka-Kudla, M.L., 1991. Coral reefs: sources or sinks of atmospheric CO_2? Coral Reefs 11, 127–130.

Wenzhofer, F., Adler, M., Kohls, O., Hensen, C., Strotmann, B., Boehme, S., Schulz, H.D., 2001. Calcite dissolution driven by benthic mineralization in the deep-sea: in situ measurements of Ca^{2+}, pH, pCO_2 and O_2. Geochim. Cosmochim. Acta 65, 2677–2690.

Wolf-Gladrow, D., Riebesell, U., 1997. Diffusion and reactions in the vicinity of plankton: a refined model for inorganic carbon transport. Mar. Chem. 59, 17–34.

Wollast, R., Garrels, R.M., MacKenzie, F.T., 1980. Calcite-seawater reactions in ocean surface waters. Am. J. Sci. 280, 831–848.

Zhang, J.-Z., 2000. The use of pH and buffer intensity to quantify the carbon cycle in the ocean. Mar. Chem. 70, 121–131.

Zeebe, R.E., Wolf-Gladrow, D., 2001. CO_2 in Seawater: Equilibrium, Kinetics, Isotopes. Elsevier oceanography Series, vol. 65. Elsevier, Amsterdam. 346 pp.